Delaying Cattle Slaughter: Dynamic Efficiency and Transition under Minimum Age Rules*

Raul A. Sosa† Franco M. Vazquez‡

Abstract

Minimum slaughter-age (or weight) rules delay harvest rather than tax quantities. We develop a continuous-time model of cattle as biological capital that maps slaughter age into harvest flow through a decreasing harvest fraction. The model yields closed-form steady states with and without a binding floor and characterizes the optimal transition after repeal. A binding floor necessarily enlarges the herd and lowers the marginal value of stock; long-run beef supply is non-monotone in the tightness of the floor—moderate floors can raise throughput, while strict floors reduce it. Repeal generates an immediate slaughter surge and monotone convergence back to the interior allocation. The framework is robust to preferences, biological growth, age-specific survival, and holding costs, and it delivers a simple sufficient-statistic measure of the policy's dynamic efficiency cost.

Keywords: Dynamic Optimization, Beef Cattle Production, Agricultural Policy
JEL Classification: Q18, C61, Q28.

*We thank Federico Sturzenegger, Joaquín Coleff and Javier García Cicco for their insightful comments and suggestions.

†Department of Economics, Universidad de San Andrés. E-mail: rsosa@udesa.edu.ar.
‡Department of Economics, Universidad de San Andrés. E-mail: vazquezf@udesa.edu.ar.

1 Introduction

Many regulations in renewable–resource sectors do not tax or cap quantities. Instead, they delay action. Minimum legal sizes in fisheries, minimum rotation ages in forestry, and minimum slaughter weights or ages in livestock operate on the timing margin, postponing harvest until a policy threshold is met. These rules are simple to administer and align with biological or ethical aims, yet they compel managers to depart from the intertemporal trade-off that would otherwise govern the use of a living stock. We study how such timing floors affect steady-state output, the size and composition of the standing stock, and the value of holding inventory, and how the system adjusts once a binding floor is removed.

Policy experience motivates our focus. In Argentina, the federal *peso mínimo de faena bovina* set sex-specific carcass thresholds of 165 kg for males and 140 kg for females, applied through a sequence of resolutions since 2007 and repealed in June 2025 with elimination effective 1 January 2026. This rule sat alongside a broader policy package: Rossini et al. (2017) analyze the 2006–2011 interventions and document chain-wide effects on prices, slaughter, and trade, while Amaro (2024) traces the legal trajectory of the minimum carcass-weight regime and details operative thresholds and implementation. Beyond cattle, Italy's industry consortia for premium hams require pigs to be at least nine months old and about 160 kg at slaughter, while Protected Designation of Origin specifications require pigs to exceed nine months and to reach 160–170 kg; Council Regulation (EC) No 1/2005 on transport and No 1099/2009 on protection at the time of killing (including lairage and stunning) frame the broader EU regime. In France, the *Label Rouge* standard for broilers mandates a minimum slaughter age of 81 days.

We develop a continuous-time model of cattle as biological capital in which the control is slaughter age and the harvest flow maps from age through a "harvest fraction" that declines with slaughter age because within-animal weight growth exhibits diminishing returns. For concreteness we impose the policy on age; because live weight is strictly increasing in age over the relevant range (formalized in Section 4), a legal weight floor $\bar{w}$ is equivalent to an age floor $\bar{a} = w^{-1}(\bar{w})$, so all steady-state and transitional results apply verbatim to weight-based rules. The model yields closed-form steady states for the unconstrained benchmark and for an economy subject to a binding minimum slaughter age or weight, and it characterizes the transition after deregulation. The logic is straightforward: biology and discounting pin down the interior stock, while a binding floor lowers the effective harvest fraction and shifts mass from flow to stock.

Three results follow. First, minimum slaughter rules *always* deepen herd capital in the long run and *always* reduce the marginal value of an additional unit of biomass. Larger herds are an intrinsic consequence of delayed slaughter, and the lower shadow value reflects reduced scarcity at the margin. Second, long-run beef supply is non-monotone in the tightness of the floor, and the Golden-Rule benchmark helps organize this result. The Golden-Rule stock is the herd size that maximizes sustainable physical output. Because the unregulated interior allocation under positive discounting sits below this benchmark, a *moderate* floor that pushes the economy toward the Golden-Rule stock raises sustainable throughput. Tightening the floor further can push the economy beyond the Golden-Rule stock and reduce throughput despite heavier animals at harvest. Put differently, whether regulation raises or lowers long-run consumption depends on whether it moves the equilibrium *closer to* or *farther from* the Golden-Rule point; the model provides simple thresholds that separate these cases. Third, when a binding rule is lifted, the optimal response features a one-time slaughter surge, driven by the backlog of over-mature

animals and a temporary reduction in the chosen slaughter age, followed by a monotone return of the herd and the shadow value to their interior levels.

Methodologically, we derive the harvest mapping from mass balance rather than headcounts times average weights, which preserves biological structure while keeping the analysis tractable. The core comparative statics rest on two primitives, namely an Euler equation and a decreasing harvest fraction, so the results are robust to alternative preferences, biological growth, age-specific survival, and holding costs. For measurement, the gap between marginal utility and the shadow value provides a sufficient statistic for the dynamic efficiency cost of a binding floor and can be calibrated with a few observable moments. The framework extends to other maturity-based rules and can be embedded in richer market environments.

Related work in livestock economics emphasizes cattle as capital and the intertemporal nature of slaughter and retention decisions, while research on the cattle cycle highlights the role of biological lags. Resource economics has analyzed timing constraints in fisheries and forestry; by bringing an age-based instrument into a continuous-time capital model, we connect these literatures and obtain formulas and empirical implications for a policy many jurisdictions actually use.

The remainder of the paper proceeds as follows. Section 3 reviews the literatures on livestock inventories, timing constraints in renewable resources, and within-animal growth. Section 4 introduces the dynamic model, the harvest fraction, and the planner's problem. Section 4.1 characterizes the unconstrained interior benchmark and gives closed-form expressions for steady-state stock, throughput, and shadow value. Section 4.2 analyzes the binding minimum slaughter-age or weight regime and derives its steady state, including the policy wedge. Section 5 compares the two regimes and identifies when timing floors raise or lower long-run output. Section 7 studies an unanticipated repeal of a binding rule and shows that the optimal adjustment features an immediate slaughter spike and monotone convergence back to the interior. Section 8 establishes robustness to preferences, biological growth, age-specific survival, holding costs, and simple price environments. Section 9 concludes with implications for policy design and avenues for empirical tests.

2 Institutional timeline and descriptive evidence

We begin with a brief overview of Argentina's minimum slaughter-weight (age) rule and a set of descriptive patterns intended to motivate the model. The timeline in Figure 1 situates three policy milestones. Figure 2 traces the long-run co-movement of slaughter and the national herd, and Figure 3 summarizes the evolution of slaughter composition by category. These patterns are presented as stylized facts to anchor the subsequent analysis.

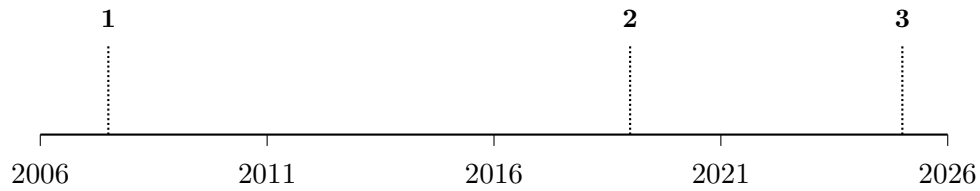

1. **2007–08 — Introduction of the minimum carcass-weight rule.** Minimum set at **99 kg per half-carcass**.
2. **2019 — Classification update / enforcement refresh.** Latest modifications (2018–2019) set sex-specific thresholds at **165 kg (males) / 140 kg (females)**.
3. **2025→26 — Repeal and elimination.** Repeal (June 2025); elimination effective **1 Jan 2026**.

Figure 1: Timeline with indexed markers

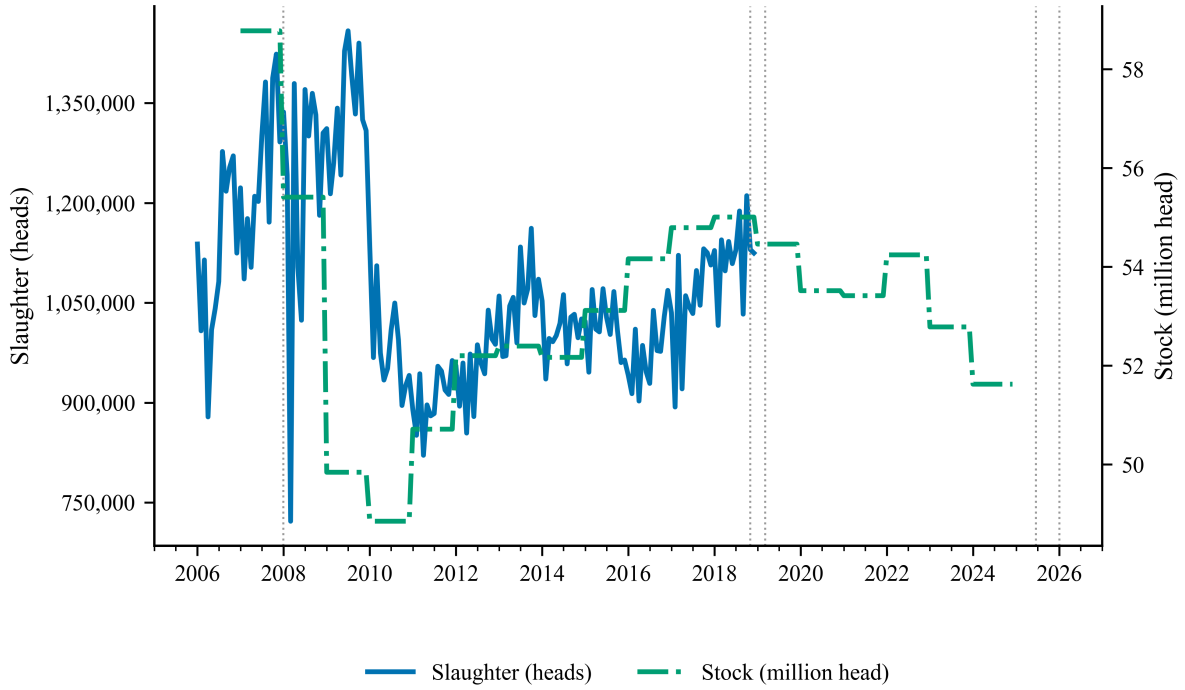

Figure 2: **Slaughter and stock (national herd).** Monthly slaughter (left axis) and annual herd stock (right axis). Dotted lines mark the policy milestones in Figure 1. Legends are placed outside the plotting area for readability.

A visual inspection of Figure 2 suggests that following the 2019 adjustment that lowered the minimum carcass-weight threshold for females from 165 kg to 140 kg, the national headcount (in millions of heads) declines, consistent with earlier slaughter and a temporary drawdown of inventories.

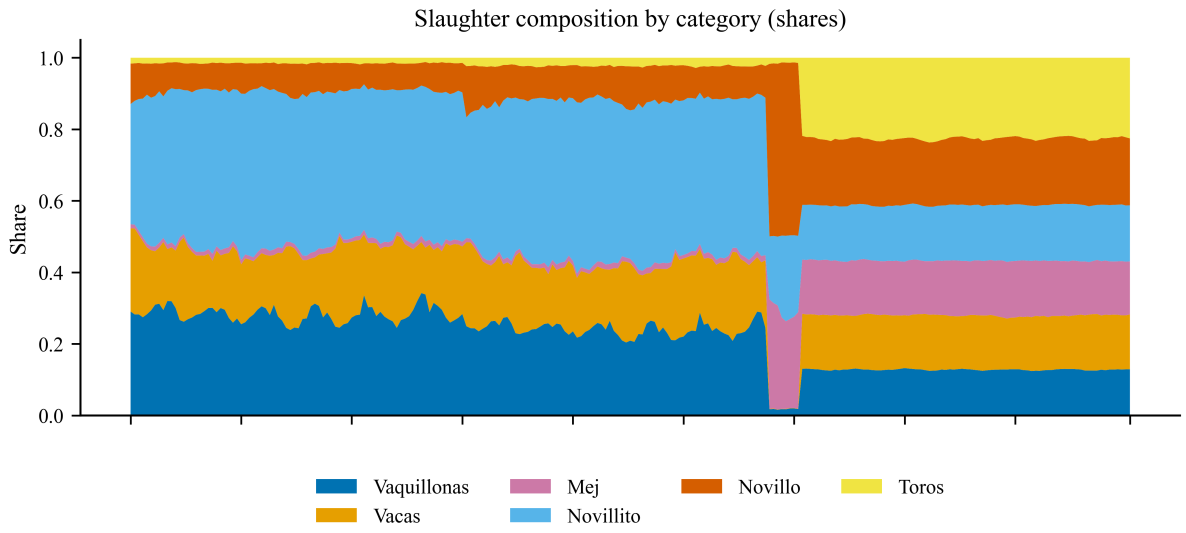

Figure 3: **Slaughter composition by category (shares).** Shares of total slaughter by category. The legend in English is: *Heifers (Vaquillonas), Cows (Vacas), Young entire male (MEJ), Young steer (Novillito), Steer (Novillo), Bulls (Toros).*

Figure 3 shows the evolution of shares of animal categories in slaughter in Argentina, between 2013 and 2022. The compositional break after the 2019 reduction in the minimum carcass-weight floor for females (from 165 kg to 140 kg) coincides with a visible reweighting of slaughter categories. The shares of animals that typically enter at younger or lower slaughter weights—*Steers* and *Young entire male*—increase, while the share of *Heifers)* declines. We also observe a rise in the share of *Bulls*, plausibly reflecting stronger incentives to retain males for breeding and to bolster reproductive capacity.

3 Literature Review

Research on the optimal management of living stocks treats herds, forests, and fisheries as forms of reproducible capital whose growth and extraction decisions unfold over time. In this tradition, a planner (or sole owner) balances the immediate gains from harvest against the foregone growth of the asset, an idea that goes back to rotation problems in forestry (Faustmann, 1849) and is formalized in modern resource economics (Clark, 2010). A prominent set of real-world interventions operates not through prices or quantities but through timing rules, such as minimum size, age, or rotation requirements, that postpone harvest until a policy threshold is reached. These rules change the age and size composition of the standing stock and can shift both long-run yields and the value of holding inventory.

Within livestock economics, the idea of cattle as capital has deep roots. Early work showed how forward-looking producers adjust slaughter and retention when market signals favor future returns, generating inverse short-run supply responses and investment-like dynamics in the herd (Jarvis, 1974). Subsequent studies embedded culling, replacement, and retention decisions in dynamic frameworks, emphasizing that changes in slaughter policy alter the composition of productive animals and the path of inventories (e.g., Rucker et al., 1984; Yager et al., 1980; Trapp, 1986; Melton, 1980; Foster and Burt, 1992). A large applied literature—especially in dairy—uses dynamic programming to map biological

states (age, yield, fertility) into culling thresholds and replacement policies, yielding implementable decision rules under uncertainty (Stewart et al., 1977; Frasier and Pfeiffer, 1994; Tronstad and Gum, 1994; Arnade and Jones, 2003; Schmitz, 1997). Together, these contributions show that slaughter and retention are intertemporal choices rather than static throughput decisions.

A complementary body of work explains the cattle cycle as the interaction of biological lags with forward-looking behavior. When breeding and finishing take time, changes in returns propagate through the age distribution of the herd, producing persistent fluctuations in slaughter, prices, and inventories (Rosen, 1987; Rosen et al., 1994). This perspective clarifies why hard timing thresholds, such as minimum slaughter ages or weights, have effects that go beyond simple quantity restrictions, because shifting the timing margin also reshapes the entire distribution of animals in the pipeline.

Outside of livestock, economics has studied timing constraints in renewable resources more explicitly. In fisheries, minimum legal size rules and selective harvesting have been analyzed with age- and stage-structured models, showing how delaying capture can raise the average size of the stock, alter steady-state yields, and in some cases change local stability (Tahvonen, 2009; Schott, 2001; Meng et al., 2013). In forestry, minimum rotation ages and ordered access constraints provide closely related benchmarks with clear implications for standing capital and sustainable output (Wan and Anderson, 1983; Płotkowski et al., 2016). Textbook treatments formalize these insights and emphasize that timing floors reallocate mass from flow to stock in steady state (Clark, 2010). Although the logic carries over to herds, comparatively few papers study minimum slaughter-age or slaughter-weight rules directly in a livestock setting and trace out their long-run consequences.

The animal-science and bioeconomic literatures provide empirical structure for how age maps into weight, carcass traits, and profitability, which is essential for evaluating timing rules. Studies comparing genotypes and production systems identify economically relevant slaughter endpoints that vary across breeds and markets, with profit peaks typically occurring between the late second and early third year of life depending on feed regimes and quality premia (Amer et al., 1994; Williams and Bennett, 1995; Kim et al., 2005; Lee et al., 2013; Lee and Lee, 2024; López-Campos et al., 2013; Pordomingo and Pordomingo, 2021). These findings discipline the shape of within-animal growth and the trade-off between throughput and average weight at harvest.

Our paper contributes to these literatures by providing a unified and testable treatment of maturity-based slaughter rules within a dynamic herd-capital framework. On the livestock side, we incorporate an explicit legal timing threshold into a model of cattle as biological capital and trace its implications for the steady state, the shadow value of stock, and the full adjustment path after repeal. On the renewable resource side, we translate size and rotation constraints to herds through a simple harvest fraction that summarizes how timing rules shift mass from flow to stock. Methodologically, the framework yields closed-form steady states, transparent viability and threshold conditions, and a stable transition with sharp empirical signatures, including a backlog-driven slaughter surge. Substantively, the main comparisons are robust to alternative preferences, biological growth profiles, age-specific survival, and basic holding costs, and the structure accommodates simple price environments. For measurement, we derive a compact statistic that captures the dynamic efficiency cost of a binding floor and show how to calibrate it with administrative records on slaughter weights and ages and a few observable moments. The framework links policy episodes, such as Argentina's carcass-weight regime, to a broader literature

on timing rules and yields predictions that can be taken to data.

4 Model

We study a continuous–time economy in which a representative manager (equivalently, a social planner in the sole–owner benchmark) chooses the slaughter age of cattle to maximize intertemporal welfare. The stock of biological capital is the total live biomass of the herd, denoted $x(t)$.

In the absence of harvesting, biomass follows logistic growth with intrinsic rate $r > 0$ and carrying capacity $K > 0$,

$$\dot{x}(t) \;=\; r\,x(t)\Big(1 - \frac{x(t)}{K}\Big)\,. \tag{1}$$

Harvesting removes biomass from the state. Let $c(t) \geq 0$ denote the outflow of biomass per unit time. The state equation with harvest is

$$\dot{x}(t) \;=\; r\,x(t)\Big(1 - \frac{x(t)}{K}\Big) \;-\; c(t)\,, \qquad x(0) = x_0 > 0. \tag{2}$$

We consider feasible paths with $x(t) \geq 0$ for all t.

The control is the slaughter age, $a(t) \in [\bar{a}, \infty)$, where $\bar{a} \geq 0$ is a legal minimum.[1] Under a fixed slaughter age a and no baseline mortality, a constant entry flow b (heads per unit time) implies a uniform age density on $[0, a]$. Biomass and outflow then satisfy

$$x \;=\; b\int_0^a w(u)\,du, \qquad c \;=\; b\,w(a).$$

It is convenient to define the effective harvest fraction,

$$\Theta(a) \;\equiv\; \frac{c}{x} \;=\; \frac{w(a)}{\displaystyle\int_0^a w(u)\,du}. \tag{3}$$

Along any path we use the reduced form $c(t) = x(t)\,\Theta\Big(a(t)\Big)$; this mapping is exact at steady states with fixed a and is a tractable aggregator off steady state.[2]

Assumptions. We assume: (i) $w(0) = 0$, $w'(u) > 0$, and $w''(u) \leq 0$ (increasing, concave within–animal weight); (ii) biological parameters $r > 0$, $K > 0$; (iii) instantaneous utility u is strictly concave with $u'(c) > 0$; (iv) discount rate $\rho > 0$.

Units. x is live biomass (kg), c is biomass outflow/consumption (kg per unit time), a is age (units of time), $w(u)$ is live weight at age u (kg), and $\Theta(a)$ is a flow–stock ratio (units of 1/time).

[1] A legal weight floor $\bar{w}$ is equivalent to an age floor $\bar{a} = w^{-1}(\bar{w})$ whenever the individual weight function $w(\cdot)$ is strictly increasing. Our analysis therefore speaks to both age and weight floors.

[2] When $a(t)$ changes, the age distribution becomes non-stationary. We retain $c = x\,\Theta(a)$ as a reduced-form mapping; Section 7 shows that transitional dynamics are governed by the Euler condition and do not hinge on tracking the full age distribution.

If $w(0) = 0$, $w'(u) > 0$, and $w''(u) \le 0$ (increasing and concave), then

$$\Theta'(a) = \frac{\left(\int_0^a w(u)\,du\right) w'(a) - w(a)^2}{\left(\int_0^a w(u)\,du\right)^2} < 0,$$

because $w'(a) \le w(a)/a$ and $\int_0^a w \ge \frac{1}{2} a\, w(a)$. A general proof is in Appendix H.5. For the canonical curve $w(u) = \frac{\alpha u}{u+k}$ the closed forms in Appendix B also imply $\Theta'(a) < 0$ (Appendix B).

Proposition 1 (Monotone harvest fraction (canonical case)). *Under the canonical growth curve $w(u) = \frac{\alpha u}{u+k}$ with $\alpha, k > 0$, the harvest fraction $\Theta(a) = \frac{w(a)}{\int_0^a w(u)\,du}$ is strictly decreasing: $\Theta'(a) < 0$ for all $a > 0$. Proof: Appendix B.* □

A positive steady state under a fixed policy requires $\Theta(a) < r$. We therefore define the viability set $\mathcal{A}_V \equiv \{a \ge \bar{a} : \Theta(a) < r\}$.[3]

Instantaneous utility is $u(c) = \sqrt{c}$ and future utility is discounted at rate $\rho > 0$. The planner chooses a measurable control $a(\cdot) \in [\bar{a}, \infty)$ to solve

$$\max_{a(\cdot)\in[\bar{a},\infty)} \int_0^\infty e^{-\rho t}\sqrt{c(t)}\,dt \quad \text{s.t.} \quad (2), \quad c(t) = x(t)\,\Theta\big(a(t)\big), \quad x(0) = x_0 > 0. \tag{4}$$

Let $\lambda(t)$ denote the current-value shadow value of biomass and $\lambda^{\mathrm{pv}}(t) = e^{-\rho t}\lambda(t)$ its present-value counterpart. We impose the standard transversality condition,

$$\lim_{t\to\infty} \lambda^{\mathrm{pv}}(t)\, x(t) \;=\; 0.$$

The current-value Hamiltonian is

$$H\big(x, a, \lambda\big) \;=\; \sqrt{c(x,a)} \;+\; \lambda\Big[r\,x\Big(1 - \frac{x}{K}\Big) - c(x,a)\Big], \qquad c(x,a) \equiv x\,\Theta(a).$$

Differentiating with respect to a and using $c = x\,\Theta(a)$ gives

$$\frac{\partial H}{\partial a} \;=\; \frac{\partial(\sqrt{c})}{\partial c}\,\frac{\partial c}{\partial a} \;-\; \lambda\,\frac{\partial c}{\partial a} \;=\; \Big(\frac{1}{2\sqrt{c}} - \lambda\Big)\,x\,\Theta'(a)\,, \tag{5}$$

or, along a path,

$$\frac{\partial H}{\partial a}(t) \;=\; x(t)\,\Theta'\big(a(t)\big)\,\Big(\frac{1}{2\sqrt{c(t)}} - \lambda(t)\Big). \tag{6}$$

With the lower bound $a(t) \ge \bar{a}$, the Kuhn–Tucker conditions are

$$\frac{\partial H}{\partial a}(t) \le 0, \qquad \mu(t) \ge 0, \qquad \mu(t)\big(a(t) - \bar{a}\big) = 0, \qquad \frac{\partial H}{\partial a}(t) + \mu(t) = 0,$$

where $\mu(t)$ is the multiplier on the control bound. Two cases emerge. If $a(t) > \bar{a}$ then $\mu(t) = 0$ and, since $x(t) > 0$ and $\Theta'(a) \ne 0$ in the relevant range,

$$\lambda(t) \;=\; \frac{1}{2\sqrt{c(t)}}. \tag{7}$$

[3] Under logistic growth $\dot{x} = r\,x(1 - x/K) - c$ and $c = x\,\Theta(a)$, a positive steady state satisfies $r(1 - x/K) = \Theta(a)$ for some $x \in (0, K)$. Thus $\Theta(a) < r$ is necessary and sufficient for a positive steady state.

If $a(t) = \bar{a}$ and $\Theta'(\bar{a}) < 0$, then (6) implies

$$\lambda(t) \;\le\; \frac{1}{2\sqrt{c(t)}} \quad \text{with strict inequality when the floor is strictly binding.} \tag{8}$$

Using $\partial c/\partial x = \Theta(a)$ and $\partial\Big[rx(1-x/K)\Big]/\partial x = r(1-2x/K)$, the derivative of the Hamiltonian with respect to x is

$$\frac{\partial H}{\partial x} \;=\; \frac{1}{2\sqrt{c}}\,\Theta(a) \;+\; \lambda\Big[r\Big(1-\frac{2x}{K}\Big) - \Theta(a)\Big],$$

so the current-value costate evolves according to

$$\dot{\lambda}(t) \;=\; \rho\,\lambda(t) \;-\; \frac{1}{2\sqrt{c(t)}}\,\Theta\Big(a(t)\Big) \;-\; \lambda(t)\Big[r\Big(1-\frac{2x(t)}{K}\Big) - \Theta\Big(a(t)\Big)\Big]. \tag{9}$$

Together, the state equation (2), the mapping $c = x\,\Theta(a)$ with the properties above, the stationarity conditions (7)–(8), the costate evolution (9), and the transversality condition characterize optimal trajectories. Subsequent analysis derives the unconstrained benchmark and the binding-floor steady state and compares their steady-state stocks, throughputs, and shadow values.

4.1 Unconstrained Benchmark (Interior Solution)

We characterize the first–best allocation when the legal floor is not binding. Formally, we analyze problem (4) under the interior condition (7). This benchmark provides the intuition and the closed forms used later to compare with the regulated outcome in Subsection 4.2 and to study post-reform transitions.

First-order condition and interior dynamics. Imposing (7),

$$\lambda(t) = \frac{1}{2\sqrt{c(t)}} \quad \text{with} \quad c(t) = x(t)\,\Theta\Big(a(t)\Big),$$

simplifies the costate equation (9) because the $\Theta(\cdot)$ terms cancel:

$$\dot{\lambda}(t) = \rho\,\lambda(t) - \lambda(t)\,r\Big(1-\frac{2x(t)}{K}\Big). \tag{10}$$

Together with the state equation (2),

$$\dot{x}(t) = r\,x(t)\Big(1-\frac{x(t)}{K}\Big) - c(t), \qquad c(t) = x(t)\,\Theta\Big(a(t)\Big), \tag{11}$$

equations (10)–(11) describe the interior dynamics. The control $a(t)$ adjusts so that (7) holds at each date. Combining $c = \frac{1}{4\lambda^2}$ with $c = x\,\Theta(a)$ gives a convenient feedback rule,

$$\Theta\Big(a(t)\Big) = \frac{1}{4\,\lambda(t)^2\,x(t)} \quad\Longrightarrow\quad a(t) = \Theta^{-1}\Big(\frac{1}{4\,\lambda(t)^2\,x(t)}\Big), \tag{12}$$

which is well defined on the viability set because Θ is continuous and strictly decreasing (Proposition 1).[4]

[4]Monotonicity implies comparative statics of the policy: holding λ fixed, a increases with x; holding x fixed, a increases with λ.

We now derive the unique interior steady state. Setting $\dot{\lambda} = 0$ in (10) (and ruling out the trivial $\lambda = 0$) yields

$$r\Big(1 - \frac{2x_I^*}{K}\Big) = \rho \quad \Longrightarrow \quad x_I^* = \frac{K}{2}\Big(1 - \frac{\rho}{r}\Big), \tag{13}$$

which requires $r > \rho$ for positivity.[5] Using $\dot{x} = 0$ in (11) gives $r(1 - x_I^*/K) = \Theta(a^*)$, hence

$$\Theta(a^*) = \frac{r+\rho}{2}. \tag{14}$$

Because Θ is strictly decreasing and $\frac{r+\rho}{2} \in (0, r)$ when $r > \rho$, (14) pins down a unique a^* in the viability set. The associated harvest and shadow value are

$$c_I^* = x_I^*\,\Theta(a^*) = \frac{K}{4r}\big(r^2 - \rho^2\big), \qquad \lambda_I^* = \frac{1}{2\sqrt{c_I^*}}. \tag{15}$$

Proposition 2 (First–best characterization)**.** *Suppose $r > \rho$ and Θ is continuous and strictly decreasing with $\lim_{a\to 0}\Theta(a) > \frac{r+\rho}{2}$ and $\lim_{a\to\infty}\Theta(a) = 0$ (satisfied by the canonical $w(\cdot)$ in Appendix A). Then there exists a unique interior steady state with*

$$x_I^* = \frac{K}{2}\Big(1 - \frac{\rho}{r}\Big), \quad \Theta(a^*) = \frac{r+\rho}{2}, \quad c_I^* = \frac{K}{4r}\big(r^2 - \rho^2\big), \quad \lambda_I^* = \frac{1}{2\sqrt{c_I^*}}.$$

Moreover a^* is unique. Proof: Appendix G.1. □

Corollary 1 (Maximum sustainable yield as $\rho \to 0$)**.** *As $\rho \to 0$, $x_I^* \to K/2$, $\Theta(a^*) \to r/2$, and $c_I^* \to rK/4$.*

Turning to comparative statics, we start from (13), which implies

$$\frac{\partial x_I^*}{\partial r} = \frac{K}{2}\frac{\rho}{r^2} > 0, \qquad \frac{\partial x_I^*}{\partial \rho} = -\frac{K}{2r} < 0,$$

so faster biological growth supports a larger interior stock, while greater impatience lowers it. Implicit differentiation of (14) using $\Theta'(a^*) < 0$ (Proposition 1) yields

$$\frac{\partial a^*}{\partial r} = \frac{1/2}{\Theta'(a^*)} < 0, \qquad \frac{\partial a^*}{\partial \rho} = \frac{1/2}{\Theta'(a^*)} < 0, \tag{16}$$

so higher r or higher ρ both imply younger optimal slaughter ages. Finally, $c_I^* = \frac{K}{4r}(r^2 - \rho^2)$ is increasing in r and decreasing in ρ for $r > \rho$:

$$\frac{\partial c_I^*}{\partial r} = \frac{K}{4}\Big(1 + \frac{\rho^2}{r^2}\Big) > 0, \qquad \frac{\partial c_I^*}{\partial \rho} = -\frac{K}{2}\frac{\rho}{r} < 0.$$

To describe local dynamics, we linearize the system (11)–(10) around (x_I^*, λ_I^*). The Jacobian has one positive and one negative eigenvalue, so the steady state is a saddle and the present-value transversality condition selects the unique stable manifold.[6] Two monotonicities follow directly from (10). When $x(t) > x_I^*$ we have $r(1 - 2x/K) < \rho$ and therefore $\dot{\lambda}(t) > 0$. When $x(t) < x_I^*$ we have $\dot{\lambda}(t) < 0$.

The interior solution provides the natural benchmark for the regulated problem. When the legal floor satisfies $\bar{a} \le a^*$, the constraint is slack and the regulated allocation coincides with the interior one. The policy-relevant case is $\bar{a} > a^*$, analyzed next.

[5] If $r \le \rho$, the interior steady state collapses to $x_I^* = 0$ under standard transversality; the empirically relevant case is $r > \rho$.

[6] Proof in Appendix G.4. (10) implies $\dot{\lambda}$ increases in x, whereas (11) implies $\dot{x}$ decreases in c and therefore *increases* in λ along the interior relation $c = 1/(4\lambda^2)$.

4.2 Regulation: Binding Minimum Slaughter Age

Consider the regime in which the legal floor binds, so the control is fixed at

$$a(t) \equiv \bar{a} \qquad \text{with} \qquad \Theta(\bar{a}) < r \quad \text{(viability)}.$$

When $\bar{a} \leq a^*$ the constraint is slack and the allocation coincides with the interior benchmark in Subsection 4.1. The policy-relevant case is $\bar{a} > a^*$, equivalently $\Theta(\bar{a}) < \frac{r+\rho}{2}$, where (8) holds with strict inequality.

With $a(t) = \bar{a}$, the outflow is $c(t) = x(t)\,\Theta(\bar{a})$ and the state equation (2) becomes

$$\dot{x}(t) = r\,x(t)\Big(1 - \frac{x(t)}{K}\Big) - x(t)\,\Theta(\bar{a}).$$

The current-value costate dynamics follow from (9) with $a(t) = \bar{a}$,

$$\dot{\lambda}(t) = \rho\,\lambda(t) - \frac{1}{2\sqrt{c(t)}}\,\Theta(\bar{a}) - \lambda(t)\Big[r\Big(1 - \frac{2x(t)}{K}\Big) - \Theta(\bar{a})\Big],$$

and the stationarity inequality (8) holds at every date with strict inequality when the floor binds:

$$\lambda(t) < \frac{1}{2\sqrt{c(t)}}, \qquad \mu(t) = -\frac{\partial H}{\partial a}(t) = -\,x(t)\,\Theta'(\bar{a})\Big(\tfrac{1}{2\sqrt{c(t)}} - \lambda(t)\Big) > 0,$$

because $\Theta'(\bar{a}) < 0$ by Proposition 1. The multiplier $\mu(t)$ is the shadow cost of the constraint and equals the Euler–equation wedge times the policy's bite: $\mu(t) = \big[-x(t)\Theta'(\bar{a})\big]\big(u'(c(t)) - \lambda(t)\big)$.

At a steady state, setting $\dot{x} = 0$ yields a unique $x_R^* \in (0, K)$ characterized by

$$r\Big(1 - \frac{x_R^*}{K}\Big) = \Theta(\bar{a}) \quad \Longleftrightarrow \quad x_R^* = K\Big(1 - \frac{\Theta(\bar{a})}{r}\Big), \tag{17}$$

and the associated throughput is

$$c_R^* = x_R^*\,\Theta(\bar{a}) = K\,\Theta(\bar{a})\Big(1 - \frac{\Theta(\bar{a})}{r}\Big). \tag{18}$$

Using $\dot{\lambda} = 0$ in the costate equation and $r(1 - 2x_R^*/K) - \Theta(\bar{a}) = -r\,x_R^*/K$ gives

$$\Big(\rho + \tfrac{r\,x_R^*}{K}\Big)\,\lambda_R^* = \frac{\Theta(\bar{a})}{2\sqrt{c_R^*}},$$

hence

$$\lambda_R^* = \frac{\Theta(\bar{a})}{2\sqrt{c_R^*}\,\big(\rho + \frac{r\,x_R^*}{K}\big)} = \frac{\sqrt{\Theta(\bar{a})}}{2\,\sqrt{x_R^*}\,(\rho + r - \Theta(\bar{a}))}. \tag{19}$$

Proposition 3 (Regulated steady state under a binding floor)**.** *If $\Theta(\bar{a}) \in (0, r)$, there exists a unique positive steady state $(x_R^*, c_R^*, \lambda_R^*)$ given by (17)–(19). As $\Theta(\bar{a}) \uparrow r$ the steady state collapses ($x_R^*, c_R^* \to 0$ and $\lambda_R^* \to \infty$); as $\Theta(\bar{a}) \downarrow 0$, we have $x_R^* \to K$, $c_R^* \to 0$, and $\lambda_R^* \to 0$. Proof: Appendix G.2.* □

Comparative statics with respect to the floor follow from (17)–(18). Because Θ is strictly decreasing, the minimum slaughter age $\bar{a}$ is a sufficient statistic for policy. Differentiating gives

$$\frac{\partial x_R^*}{\partial \bar{a}} = -\frac{K}{r}\,\Theta'(\bar{a}) > 0, \tag{20}$$

so tighter floors increase the standing herd (capital deepening). For throughput,

$$\frac{\partial c_R^*}{\partial \bar{a}} = K\,\Theta'(\bar{a})\Big(1 - \frac{2\,\Theta(\bar{a})}{r}\Big), \tag{21}$$

which is positive when $\Theta(\bar{a}) > \frac{r}{2}$ and negative when $\Theta(\bar{a}) < \frac{r}{2}$. Hence c_R^* is single-peaked in $\bar{a}$ (equivalently, in Θ), with a maximum at the biological MSY point $\Theta(\bar{a}) = r/2$. Using (19) and treating λ_R^* as a function of $\Theta \in (0, r)$,

$$\lambda_R^*(\Theta) = \frac{\sqrt{\Theta}}{2\sqrt{K(1-\Theta/r)}\,(\rho + r - \Theta)}.$$

A direct derivative shows $d\lambda_R^*/d\Theta > 0$ on $(0, r)$ (Lemma 5 in Appendix G). With $\Theta'(\bar{a}) < 0$ this implies

$$\frac{\partial \lambda_R^*}{\partial \bar{a}} = \frac{d\lambda_R^*}{d\Theta}\,\Theta'(\bar{a}) < 0. \tag{22}$$

Thus tighter floors lower the marginal value of biomass at the regulated steady state.

It is useful to summarize the distortion with a steady-state wedge,

$$\Delta_R^* \equiv \frac{1}{2\sqrt{c_R^*}} - \lambda_R^*,$$

which vanishes at the interior optimum and is positive under a binding floor. Combining (19) with $r\,x_R^*/K = r - \Theta(\bar{a})$ yields

$$\Delta_R^* = \frac{\rho + r - 2\,\Theta(\bar{a})}{\rho + r - \Theta(\bar{a})} \cdot \frac{1}{2\sqrt{c_R^*}}, \tag{23}$$

strictly positive if and only if $\Theta(\bar{a}) < \frac{r+\rho}{2}$ and increasing as $\Theta(\bar{a})$ falls. The associated multiplier is

$$\mu_R^* = -\,x_R^*\,\Theta'(\bar{a})\,\Delta_R^* > 0, \tag{24}$$

so the wedge scales one-for-one with the shadow cost of the constraint, adjusted by the policy's bite $-x_R^*\,\Theta'(\bar{a})$.

For local stability, we linearize the (x, λ) system with $a(t) \equiv \bar{a}$ at (x_R^*, λ_R^*). The Jacobian has one positive and one negative eigenvalue; the steady state is a saddle and the present-value transversality condition selects the unique stable arm.[7]

5 Steady-State Comparison

We compare the interior benchmark in Subsection 4.1 with the regulated outcome in Subsection 4.2. Throughout we focus on the policy-relevant case in which the legal floor *binds*, i.e. $\bar{a} > a^*$, or equivalently (by (14)) $\Theta(\bar{a}) < \frac{r+\rho}{2}$.[8]

[7] Write $\dot{x} = f(x) \equiv rx(1 - x/K) - x\Theta(\bar{a})$, so $f'(x_R^*) = r(1 - 2x_R^*/K) - \Theta(\bar{a}) = -rx_R^*/K < 0$. From the costate equation with fixed a, $\partial\dot{\lambda}/\partial\lambda|_{(x_R^*, \lambda_R^*)} = \rho - (r(1 - 2x_R^*/K) - \Theta(\bar{a})) = \rho + rx_R^*/K > 0$. The determinant is negative (Appendix G.4).

[8] We also maintain the viability condition for a regulated steady state, $\Theta(\bar{a}) \in (0, r)$.

Recall the steady-state characterizations. From (13)–(15),

$$x_I^* = \frac{K}{2}\left(1 - \frac{\rho}{r}\right), \quad \Theta(a^*) = \frac{r+\rho}{2}, \quad c_I^* = x_I^*\,\Theta(a^*), \quad \lambda_I^* = \frac{1}{2\sqrt{c_I^*}}.$$

From (17)–(19),

$$x_R^* = K\left(1 - \frac{\Theta(\bar{a})}{r}\right), \quad c_R^* = x_R^*\,\Theta(\bar{a}), \quad \lambda_R^* = \frac{\sqrt{\Theta(\bar{a})}}{2\sqrt{x_R^*}\,(\rho + r - \Theta(\bar{a}))}.$$

Proposition 4 (Capital deepening and lower marginal value)**.** *If the floor binds ($\bar{a} > a^*$), then*

$$x_R^* > x_I^* \qquad \text{and} \qquad \lambda_R^* < \lambda_I^*.$$

Proof. *$x_R^* > x_I^*$ iff $\Theta(\bar{a}) < \frac{r+\rho}{2}$ (Appendix C). Given $\bar{a} > a^*$ (equivalently $\Theta(\bar{a}) < \frac{r+\rho}{2}$), Appendix D shows $\lambda_R^* < \lambda_I^*$, with equality only when $\bar{a} = a^*$ (non-binding).* □

A binding floor forces biomass to accumulate (capital deepening) in order to sustain a lower harvest fraction $\Theta(\bar{a})$. At the larger stock, the marginal value of an extra unit of biomass is lower.

Proposition 5 (When the floor raises long-run output)**.** *Let c_R^* and c_I^* be given by (18) and (15). Then*

$$c_R^* \begin{cases} > c_I^*, & \text{iff } \dfrac{r-\rho}{2} < \Theta(\bar{a}) < \dfrac{r+\rho}{2}, \\ = c_I^*, & \text{if } \Theta(\bar{a}) \in \left\{\dfrac{r-\rho}{2}, \dfrac{r+\rho}{2}\right\}, \\ < c_I^*, & \text{otherwise.} \end{cases}$$

Proof. *Rearranging $c_R^* > c_I^*$ yields the quadratic $4\Theta^2 - 4r\Theta + (r^2 - \rho^2) < 0$ in $\Theta \equiv \Theta(\bar{a})$, whose roots are $\frac{r\pm\rho}{2}$ (Appendix E).* □

Remark 1 (Endpoints and binding). At $\Theta(\bar{a}) = \frac{r+\rho}{2}$ we have $a = \bar{a} = a^*$, so the floor is slack and $c_R^* = c_I^*$. At $\Theta(\bar{a}) = \frac{r-\rho}{2}$ the floor is (strictly) binding but $c_R^* = c_I^*$. Inside the open interval $\left(\frac{r-\rho}{2}, \frac{r+\rho}{2}\right)$, a binding floor raises long-run throughput; outside it, the floor lowers throughput.

Headcount comparisons follow from the identity $N = x/\overline{w}(a)$ under a uniform age distribution and the canonical mapping between $\overline{w}$ and Θ.

Corollary 2 (Herd size in headcount)**.** *Assume the canonical weight curve $w(u) = \frac{\alpha u}{u+k}$ and a uniform age distribution at steady state. If $\bar{a} > a^*$, then $N_R^* > N_I^*$.* Proof. *Appendix F.* □

To compare welfare at the regime level, note that when $\bar{a} > a^*$ the regulated problem maximizes over a strict subset of the feasible controls relative to the interior benchmark; hence the regulated optimum is (weakly) dominated by the interior one. The formal statement, the wedge–bite decomposition, and the monotone sensitivity of welfare to $\bar{a}$ are given in Proposition 6.

We also classify the regulated steady state relative to the golden-rule stock $x^{\mathrm{GR}} = K/2$, which maximizes sustainable physical output $c_{\max} = rK/4$ when $\rho = 0$.

Corollary 3 (Dynamic (in)efficiency under the floor)**.** *At the regulated steady state,*

$$x_R^* \gtrless \frac{K}{2} \quad \Longleftrightarrow \quad \Theta(\bar{a}) \lesseqgtr \frac{r}{2}.$$

Equivalently, $c_R^* \leq c_{\max}$ *with equality iff* $\Theta(\bar{a}) = \frac{r}{2}$. Proof. *From* (17)*:* $x_R^* > K/2$ *iff* $1 - \Theta(\bar{a})/r > 1/2$ *iff* $\Theta(\bar{a}) < r/2$*. The throughput statement follows from* (18)*, a concave quadratic in* Θ *with maximum at* $r/2$*.* □

Two implications for transition dynamics follow. If the binding floor places the economy in an over-accumulated region ($x_R^* > K/2$), deregulation can raise long-run throughput (Proposition 5, left inequality) and will generate a one-time slaughter surge followed by convergence to c_I^* (Section 7). If the floor is only mildly binding, long-run throughput may fall after deregulation despite the transitory output jump.

6 Welfare Implications

Proposition 6 (Welfare under a binding floor: ordering, monotonicity, and sensitivity)**.** *Let* $V^*(\bar{a})$ *denote the optimal value of problem* (4) *when the control is restricted by* $a(t) \geq \bar{a}$ *for all* $t \geq 0$*. Under the standing assumptions (strict concavity of* $u(\cdot)$*, feasibility and* normality *of the Maximum Principle, and a strictly decreasing harvest fraction* $\Theta'(\cdot) < 0$*), the following hold:*

(i) Strict welfare loss. *If the floor binds (equivalently, the unconstrained interior choice satisfies* $a^* < \bar{a}$*), then*

$$V^*(\bar{a}) \;<\; V^*_{\text{int}},$$

with equality if and only if the floor is slack ($\bar{a} = a^*$*).*

(ii) Welfare monotonicity in the policy. *The optimal value* $V^*(\bar{a})$ *is strictly decreasing in* $\bar{a}$*. Moreover, the one-sided derivative with respect to the policy parameter exists and satisfies the envelope identity*

$$\frac{dV^*(\bar{a})}{d\bar{a}} \;=\; -\int_0^\infty e^{-\rho t}\,\mu^*(t;\bar{a})\,dt \;<\; 0,$$

where $\mu^*(t;\bar{a})$ *is the* current-value *Lagrange multiplier on the constraint* $a(t) \geq \bar{a}$ *along the regulated optimum. Thus the integrand* $e^{-\rho t}\mu^*(t;\bar{a})$ *is the* present value *of the current-value multiplier.*

(iii) Wedge–bite decomposition. *At any date* t *at which the floor binds,*

$$\mu^*(t;\bar{a}) \;=\; -\frac{\partial H}{\partial a}(t) \;=\; -\,x(t)\,\Theta'(\bar{a})\,\big(u'(c(t)) - \lambda(t)\big) \;=\; \underbrace{\big[-\,x(t)\,\Theta'(\bar{a})\big]}_{\textit{policy bite}} \cdot \underbrace{\Delta(t)}_{\textit{wedge } u'(c)-\lambda} \;>\; 0,$$

where H *is the current-value Hamiltonian,* $\lambda(t)$ *is the current-value shadow value of biomass, and* $\Delta(t) \equiv u'(c(t)) - \lambda(t)$ *measures the instantaneous Euler-equation distortion. At the regulated steady state,* $\Delta(t) = \Delta_R^*$ *from* (23)*.*

The envelope identity in (ii) follows from standard sensitivity results for optimal control with parameterized inequality constraints; see Seierstad and Sydsæter (1987); Kamien and Schwartz (1991); Stokey et al. (1989). For interpretation in renewable-resource settings, see Clark (2010).

Proposition 7 (Welfare gain from full repeal: exact integral representation)**.** *Fix an initial biomass x_0 and let $V(x_0;\bar{a})$ denote the optimal value of problem (4) when the control is restricted by $a(t) \geq \bar{a}$ for all $t \geq 0$. Consider a one-time repeal at $t = 0$ that removes the floor permanently, so the post-repeal allocation is the unconstrained interior path (which converges to the unique interior steady state with $a(t) \to a^*$). Then the welfare gain from repeal equals*

$$\Delta V(x_0; \bar{a} \to a^*) \;\equiv\; V(x_0; a^*) - V(x_0; \bar{a}) \;=\; \int_{a^*}^{\bar{a}} \left[\int_0^{\infty} e^{-\rho t}\, \mu^*(t; \tilde{a}, x_0)\, dt \right] d\tilde{a}, \tag{25}$$

where, for each parameter value $\tilde{a} \in [a^*, \bar{a}]$, the inner integral is the present value of the current-value *Lagrange multiplier $\mu^*(t; \tilde{a}, x_0)$ on the constraint $a(t) \geq \tilde{a}$ along the* regulated *optimal path for that parameter, starting from the common initial condition x_0. Under the same regularity conditions as above (normality, measurability, and integrability), the exchange of differentiation and integration is valid.*

Moreover, at any date t where the floor binds under $\tilde{a}$,

$$\mu^*(t; \tilde{a}, x_0) \;=\; -\frac{\partial H}{\partial a}(t) \;=\; -\,x(t)\,\Theta'(\tilde{a})\,\Big(u'(c(t)) - \lambda(t)\Big) \;>\; 0,$$

so the integrand in (25) is strictly positive on a set of positive measure whenever the floor is binding. Hence $\Delta V(x_0; \bar{a} \to a^*) > 0$.

Interpretation. The welfare gain from repeal is the *area under* $e^{-\rho t}\mu^*(t; \tilde{a}, x_0)$, i.e., the present value of the current-value multiplier, as the policy parameter is relaxed from $\bar{a}$ down to a^*, holding the initial state fixed. The multiplier decomposes into the *policy bite* $\big[-x(t)\Theta'(\tilde{a})\big]$ and the *Euler-equation wedge* $\Big(u'(c(t)) - \lambda(t)\Big)$.

Corollary 4 (Path–difference expression for the welfare gain from repeal)**.** *Fix an initial state x_0. Let $(x^{\mathrm{reg}}(t), c^{\mathrm{reg}}(t), a^{\mathrm{reg}}(t))$ denote the* regulated *optimal path for the policy parameter $\bar{a}$ starting from x_0 (so $a^{\mathrm{reg}}(t) \equiv \bar{a}$ when the floor binds). Let $(x^{\mathrm{free}}(t), c^{\mathrm{free}}(t), a^{\mathrm{free}}(t))$ denote the* unconstrained *optimal path from the same x_0 (which satisfies $a^{\mathrm{free}}(0^+) < a^*$ and $a^{\mathrm{free}}(t) \to a^*$). Then the welfare gain from fully removing the floor at $t = 0$ equals*

$$\Delta V(x_0; \bar{a} \to a^*) \;=\; \int_0^{\infty} e^{-\rho t} \left[u\Big(c^{\mathrm{free}}(t)\Big) \;-\; u\Big(c^{\mathrm{reg}}(t)\Big) \right] dt.$$

Hence the full transitional dynamics of $a^{\mathrm{free}}(t)$ after repeal are part of the welfare calculation; see Section 7 for the monotone adjustment of $(x(t), \lambda(t), c(t))$.

Remark 2 (Equivalence to the multiplier–integral formula). The expression in Corollary 4 is equivalent to the integral representation in Proposition 7:

$$\Delta V(x_0; \bar{a} \to a^*) \;=\; \int_{a^*}^{\bar{a}} \left[\int_0^{\infty} e^{-\rho t}\, \mu^*(t; \tilde{a}, x_0)\, dt \right] d\tilde{a},$$

where $\mu^*(t; \tilde{a}, x_0)$ is the current-value multiplier along the *regulated* optimal path for parameter $\tilde{a}$. The multiplier admits the wedge–bite decomposition $\mu^*(t; \tilde{a}, x_0) = \big[-x(t)\Theta'(\tilde{a})\big]\,[u'(c(t)) - \lambda(t)]$. Both representations deliver the same ΔV; the former spells out the two actual paths, the latter computes the same gap by integrating the shadow price of the constraint over the policy range.

7 Policy Experiment and Transitional Dynamics

We study a one–time, unanticipated repeal at $t = 0$ that removes the minimum slaughter–age floor. Before $t = 0$, the economy is at the regulated steady state (x_R^*, λ_R^*) characterized in Section 4.2, with $a(t) \equiv \bar{a}$ binding, $\Theta(\bar{a}) < \frac{r+\rho}{2}$, and $x_R^* > x_I^*$ (Proposition 4). At $t = 0^+$ the control set expands to $a(t) \in (0, \infty)$ and the interior stationarity condition becomes admissible.

Exact age structure and backlog removal. Let $n(t, u)$ denote the headcount density by age and $w(u)$ the live weight at age u. The pre-repeal regulated steady state features a uniform age density $n(0^-, u) \equiv b^*$ on $[0, \bar{a}]$ (Appendix A). At repeal, the slaughter threshold drops from $\bar{a}$ to a new choice $a(0^+) < \bar{a}$. The McKendrick–von Foerster (MvF) boundary is absorbing; the over-age mass $u \in (a(0^+), \bar{a}]$ is harvested instantaneously, producing a discrete drop in biomass,

$$\Delta x \;=\; \int_{a(0^+)}^{\bar{a}} w(u)\, n(0^-, u)\, du \;=\; b^* \int_{a(0^+)}^{\bar{a}} w(u)\, du, \qquad x(0^+) \;=\; x(0^-) - \Delta x. \tag{26}$$

Immediately after the impulse, $n(0^+, u) \equiv b^*$ on $[0, a(0^+)]$. For $t > 0$, the *continuous* harvest flow equals the MvF boundary flux

$$c(t) \;=\; w\Big(a(t)\Big)\,\Big(1 - \dot{a}(t)\Big)_+\, n\Big(t, a(t)^-\Big), \tag{27}$$

so if $\dot{a}(0^+) < 0$ (threshold still moving down), the factor $(1 - \dot{a}(0^+)) > 1$ amplifies the immediate post-repeal slaughter flow.

Initial optimality conditions. From $t = 0^+$ onward the interior FOC holds: $\lambda(t) = u'(c(t))$; under $u(c) = \sqrt{c}$,

$$\lambda(t) = \frac{1}{2\sqrt{c(t)}}. \tag{28}$$

Under standard regularity (no discrete jump cost at repeal), the current-value costate is continuous, so

$$\lambda(0^+) = \lambda_R^*, \qquad c(0^+) = \frac{1}{4\,\lambda_R^{*2}}. \tag{29}$$

Because a binding floor implies $\lambda_R^* < \frac{1}{2\sqrt{c_R^*}}$ and Proposition 4 gives $\lambda_R^* < \lambda_I^*$, we obtain

$$c(0^+) \;>\; c_R^*, \qquad c(0^+) \;>\; c_I^*,$$

so repeal triggers an immediate slaughter surge.[9]

Proposition 8 (Impulse backlog removal and initial control). *At $t = 0$ the planner removes $\Delta x = b^* \int_{a(0^+)}^{\bar{a}} w(u)\, du$ as in (26) and chooses $a(0^+) < \bar{a}$ so that the interior FOC holds at 0^+ with $\lambda(0^+) = \lambda_R^*$ and $c(0^+) = 1/(4\lambda_R^{*2}) > \max\{c_R^*, c_I^*\}$. Moreover, evaluating $\partial H/\partial a = x\,\Theta'(a)\Big(\frac{1}{2\sqrt{c}} - \lambda\Big)$ at $a = a^*$ with $(x, \lambda) = (x(0^+), \lambda_R^*)$ yields $\frac{\partial H}{\partial a} < 0$, so $a(0^+) < a^*$. Proof: Appendix G.3.*

[9] Equation (27) shows how this can occur even when $a(0^+) < \bar{a}$: with $n(0^+, a(0^+)^-) = b^*$ and $\dot{a}(0^+) < 0$, the factor $(1 - \dot{a}(0^+)) > 1$ raises the boundary flux above $b^* w(\bar{a}) = c_R^*$.

Stable-arm landing and dynamics after repeal. For $t > 0$ the aggregate interior system

$$\dot{x}(t) = r\,x(t)\Big(1 - \frac{x(t)}{K}\Big) - c(t), \qquad \dot{\lambda}(t) = \lambda(t)\Big[\rho - r\Big(1 - \frac{2x(t)}{K}\Big)\Big], \qquad \lambda(t) = \tfrac{1}{2\sqrt{c(t)}},$$

has a saddle at (x_I^*, λ_I^*) with a unique stable arm (Appendix G.4). The jump choice $a(0^+)$ fixes $x(0^+)$ via (26). The optimal pair $(x(0^+), \lambda(0^+)) = (x(0^+), \lambda_R^*)$ must lie on the interior *stable arm*, which selects the trajectory satisfying the present-value transversality condition.

Lemma 1 (Stable-arm landing and sign of the slope). The stable arm is locally downward sloping at (x_I^*, λ_I^*). Hence, for any $\lambda(0^+) = \lambda_R^* < \lambda_I^*$, the unique point on the stable arm with that co-state satisfies $x(0^+) > x_I^*$. Proof: Appendix G.3.

Proposition 9 (Monotone transition after repeal). *Along the optimal post-repeal path,*

$$x(t) \searrow x_I^*, \qquad \lambda(t) \nearrow \lambda_I^*.$$

Differentiating $\lambda = 1/(2\sqrt{c})$ *gives* $\lambda\,\dot{c} = -2c\,\dot{\lambda}$ *and therefore*

$$\dot{c}(t) = -\,2\,c(t)\Big[\rho - r\Big(1 - \frac{2x(t)}{K}\Big)\Big] \;<\; 0 \quad \textit{for all } t \geq 0, \tag{30}$$

so $c(t)$ *declines monotonically from* $c(0^+) = 1/(4\lambda_R^{*2})$ *to* c_I^*. *Proof: Appendix G.3.* □

Comparison to the pre-repeal flow. Because $c(0^+) > c_R^*$ and $c(t) \downarrow c_I^*$, the entire transition stays above c_R^* if and only if $c_I^* \geq c_R^*$ (under a binding floor this is equivalent to $\Theta(\bar{a}) \leq \frac{r-\rho}{2}$, with equality at the endpoint; see Proposition 5). If $c_I^* < c_R^*$—i.e., when $\frac{r-\rho}{2} < \Theta(\bar{a}) < \frac{r+\rho}{2}$—there exists a unique $\hat{t} > 0$ such that $c(\hat{t}) = c_R^*$ and $c(t) < c_R^*$ for $t > \hat{t}$.

Illustrative phase diagrams and consumption paths. Figures 4 and 5 visualize the two regimes emphasized above. Panel (a) shows the (x, λ) phase portrait; panel (b) shows the corresponding path of $c(t)$. In both regimes, the post-repeal path lands on the stable arm and converges monotonically to (x_I^*, λ_I^*), with $c(t)$ declining to c_I^* (Proposition 9).

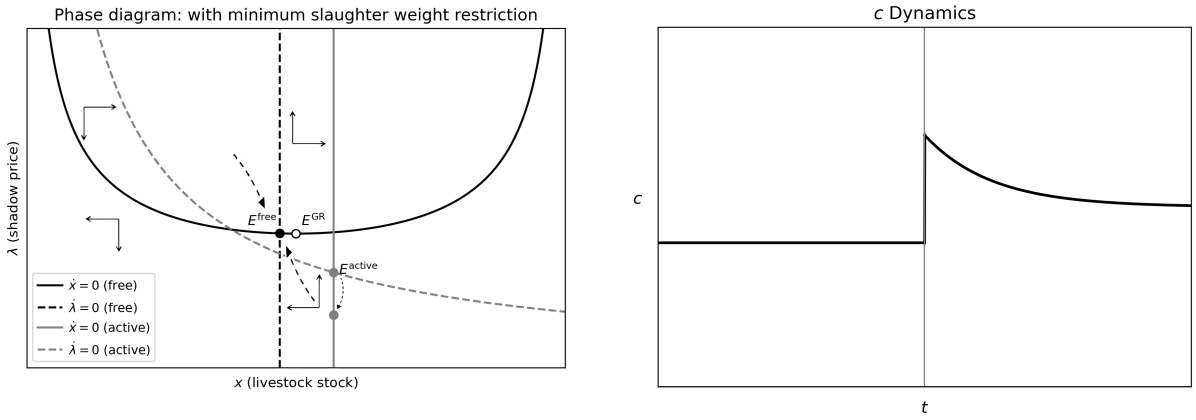

(a) Phase diagram in (x, λ) space.

(b) Consumption path $c(t)$.

Figure 4: Case $c_I^* > c_R^*$. The post-repeal (x, λ) state lands on the stable arm and converges to (x_I^*, λ_I^*); the harvest flow declines monotonically from $c(0^+)$ to c_I^*.

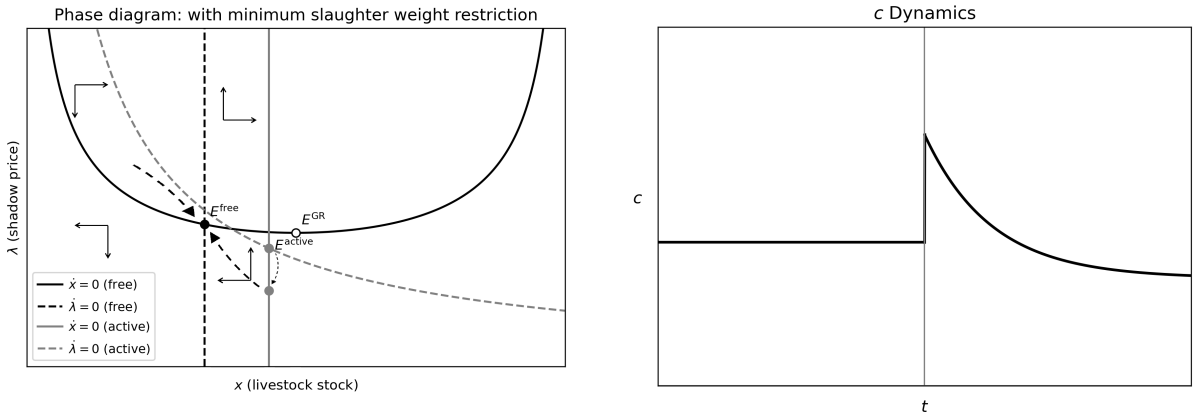

(a) Phase diagram in (x, λ) space.

(b) Consumption path $c(t)$.

Figure 5: Case $c_I^* < c_R^*$. The path lands on the stable arm and $c(t)$ declines monotonically from $c(0^+)$ to c_I^*, crossing c_R^* once.

Remark 3 (Transient controls need not satisfy $\Theta(a) < r$). The "viability set" $\{\Theta(a) < r\}$ is a *steady-state* requirement for fixed a. It is not imposed on transient controls. Consequently, the post-jump $a(0^+)$ and any short-run policy with $\dot{a}(0^+) < 0$ do not violate feasibility of the aggregate system; they simply imply rapid initial decumulation driven by the boundary flux (27).

8 Extensions and Robustness

This section examines whether the steady–state comparisons between the regulated (binding floor) and interior solutions survive changes in preferences, biological growth, and simple frictions. Throughout, let $g : [0, K] \to \mathbb{R}_+$ be increasing and strictly concave with $g(0) = g(K) = 0$, and define $h(x) \equiv g(x)/x$ on $(0, K]$, which is strictly decreasing (and $h(0^+) \equiv \lim_{x \downarrow 0} g(x)/x = g'(0^+)$ by concavity). The interior steady state satisfies

$$g'(x_I^*) = \rho, \qquad \Theta(a^*) = h(x_I^*), \qquad c_I^* = x_I^* \Theta(a^*) = g(x_I^*), \qquad \lambda_I^* = u'(c_I^*).$$

With a binding floor $a = \bar{a}$ (so $\Theta(\bar{a}) < \Theta(a^*)$), the regulated steady state solves

$$h(x_R^*) = \Theta(\bar{a}), \qquad c_R^* = x_R^* \Theta(\bar{a}) = g(x_R^*), \qquad \lambda_R^* = \frac{u'(c_R^*)\,\Theta(\bar{a})}{\rho - g'(x_R^*) + \Theta(\bar{a})}.$$

Under a binding floor we have $x_R^* > x_I^*$, hence $g'(x_R^*) < g'(x_I^*) = \rho$, so the denominator in λ_R^* is strictly positive.

The last identity comes from the steady–state costate equation and implies a policy wedge,

$$\Delta_R^* \;\equiv\; u'(c_R^*) - \lambda_R^* \;=\; u'(c_R^*)\,\frac{\rho - g'(x_R^*)}{\rho - g'(x_R^*) + \Theta(\bar{a})} \;>\; 0. \tag{31}$$

For the logistic benchmark $g(x) = rx(1 - x/K)$ we have $g'(x_R^*) = 2\Theta(\bar{a}) - r$, and (31) becomes

$$\Delta_R^* \;=\; u'(c_R^*)\,\frac{\rho + r - 2\Theta(\bar{a})}{\rho + r - \Theta(\bar{a})}.$$

Proposition 10 (Utility-robust interior benchmark). *Under the interior FOC* $u'(c) = \lambda$, *the* $\Theta(\cdot)$ *terms drop from the costate,* $\dot{\lambda} = \lambda(\rho - g'(x))$. *The unique interior steady state satisfies* $g'(x_I^*) = \rho$ *and* $\Theta(a^*) = h(x_I^*)$, *with* $c_I^* = g(x_I^*)$ *and* $\lambda_I^* = u'(c_I^*)$. Proof: *Appendix H.1.* □

Three sets of comparisons are convenient when the floor binds. (a) *Stock (biomass):* because h is decreasing and $\Theta(\bar{a}) < h(x_I^*)$ (binding), it follows that $x_R^* > x_I^*$, so capital deepening is robust. (b) *Throughput (consumption/harvest):* let x^{GR} maximize $g(x)$ (i.e., $g'(x^{\mathrm{GR}}) = 0$) and let $x_+ > x^{\mathrm{GR}}$ be the unique point with $g(x_+) = g(x_I^*)$. Then

$$c_R^* > c_I^* \iff x_R^* \in (x_I^*, x_+) \iff \Theta(\bar{a}) \in \Big(h(x_+),\, h(x_I^*)\Big).$$

For the logistic case, $h(x_I^*) = (r+\rho)/2$ and $h(x_+) = (r-\rho)/2$, so $c_R^* > c_I^*$ iff $\Theta(\bar{a}) \in \Big((r-\rho)/2,\, (r+\rho)/2\Big)$. (c) *Shadow value:* from (31), $\lambda_R^* = \dfrac{u'(c_R^*)\,\Theta(\bar{a})}{\rho - g'(x_R^*) + \Theta(\bar{a})} < u'(c_R^*)$. Hence $c_R^* \geq c_I^*$ implies $\lambda_R^* < \lambda_I^*$ since u' is decreasing. If $c_R^* < c_I^*$, the ranking depends on curvature; under CRRA $u(c) = \frac{c^{1-\sigma}}{1-\sigma}$ the inequality $\lambda_R^* < \lambda_I^*$ is satisfied whenever

$$\sigma \;<\; \frac{\ln\Big(\frac{\rho - g'(x_R^*) + \Theta(\bar{a})}{\Theta(\bar{a})}\Big)}{\ln\Big(\frac{c_I^*}{c_R^*}\Big)},$$

and in particular holds for all $\sigma > 0$ when $c_R^* \geq c_I^*$.

Proposition 11 (General growth: interior and regulated steady states). *With* $u'(c) = \lambda$ *interiorly, the unique interior steady state solves* $g'(x_I^*) = \rho$ *and* $\Theta(a^*) = h(x_I^*) = g(x_I^*)/x_I^*$. *Under a binding floor* $a = \bar{a}$, *the regulated steady state solves* $h(x_R^*) = \Theta(\bar{a})$ *and exists uniquely whenever* $\Theta(\bar{a}) \in (0, h(0^+))$ *(with* $h(0^+) = g'(0^+)$*).* Proof: *Appendix H.2.* □

Proposition 12 (Comparative statics under general growth). *If the floor binds, then* $x_R^* > x_I^*$ *iff* $\Theta(\bar{a}) < h(x_I^*)$; *and* $c_R^* > c_I^*$ *iff* $\Theta(\bar{a}) \in \Big(h(x^{\mathrm{GR}}),\, h(x_I^*)\Big)$. *The shadow-value conclusions above carry over.* Proof: *Appendix H.2.* □

Holding or feeding costs can be incorporated by writing the current-value Hamiltonian as $u(c) - \phi(x) + \lambda[g(x) - c]$ with $\phi'(x) \geq 0$. Interiorly,

$$g'(x_I^*) = \rho + \frac{\phi'(x_I^*)}{\lambda_I^*},$$

so x_I^* and $c_I^* = g(x_I^*)$ both fall, while $\Theta(a^*) = g(x_I^*)/x_I^*$ rises and optimal slaughter ages fall. At the regulated steady state (with fixed $\bar{a}$),

$$\big(\rho - g'(x_R^*) + \Theta(\bar{a})\big)\,\lambda_R^* \;=\; u'(c_R^)\,\Theta(\bar{a}) \;-\; \phi'(x_R^*),$$

which leaves (x_R^*, c_R^*) unchanged but lowers λ_R^* as $\phi'(x_R^*)$ increases. Three implications follow: the gap $x_R^* - x_I^*$ widens, the region where $c_R^* > c_I^*$ expands, and the inequality $\lambda_R^* < \lambda_I^*$ becomes strictly stronger.

Price environments and open access. With constant output price $p > 0$ and no holding costs, set $u(c) = p\,c$. Then $u'(c) = p$ implies $\lambda_I^* = p$, $g'(x_I^*) = \rho$, $\Theta(a^*) = h(x_I^*)$, and $c_I^* = g(x_I^*)$, so the interior allocation coincides with the planner's benchmark. Under a binding floor,

$$\lambda_R^* = \frac{p\,\Theta(\bar{a})}{\rho - g'(x_R^*) + \Theta(\bar{a})} \;<\; p = \lambda_I^*,$$

so $\lambda_R^* < \lambda_I^*$ holds unconditionally, and the x– and c–comparisons remain as above. With free entry, let $u(c) = p\,c - \kappa(c)$; the interior FOC becomes $p - \kappa'(c) = \lambda$ and the Euler equation is unchanged. Open access (zero profit) pins down $p = \kappa(c)/c$ in steady state, which selects c^* (hence $\Theta(a^*)$) without altering the qualitative rankings.

Age-specific survival. Let survival be $s(u) = e^{-\mu u}$ with $\mu \geq 0$. For slaughter at age a,

$$x = b \int_0^a e^{-\mu u} w(u)\,du, \qquad c = b\,e^{-\mu a} w(a),$$

so the effective harvest fraction becomes $\Theta_\mu(a) = \dfrac{e^{-\mu a} w(a)}{\int_0^a e^{-\mu u} w(u)\,du}$. If w is increasing, concave, and $w(0) = 0$, then $\Theta'_\mu(a) < 0$ for all $a > 0$, and all comparisons above go through. *Proof:* Appendix H.3. □

Alternative weight curves. The canonical $w(u) = \frac{\alpha u}{u+k}$ delivers $\Theta'(a) < 0$ in closed form. More generally, if $w(0) = 0$, $w'(u) > 0$, and $w''(u) \leq 0$, then

$$\Theta(a) = \frac{w(a)}{\int_0^a w(u)\,du} \quad \text{is strictly decreasing,}$$

so the policy variable $\bar{a}$ remains a monotone surrogate for $\Theta(\bar{a})$. Threshold statements expressed in terms of $\Theta(\bar{a})$—for example, the rules for $x_R^* \gtrless x_I^*$, $c_R^* \gtrless c_I^*$, and $\lambda_R^* \gtrless \lambda_I^*$—are therefore independent of the parametric choice of $w(\cdot)$.

Across these extensions, three comparison principles persist: $x_R^* > x_I^*$ (capital deepening), $c_R^* > c_I^*$ exactly when $\Theta(\bar{a}) \in \big(h(x_+),\, h(x_I^*)\big)$, and $\lambda_R^* < \lambda_I^*$ whenever $c_R^* \geq c_I^*$.

For the logistic–$\sqrt{\cdot}$ benchmark used in the main text, these specialize to

$$\Theta(a^*) = \frac{r+\rho}{2}, \qquad h(x^{\mathrm{GR}}) = \frac{r}{2}$$

$$c_R^* > c_I^* \iff \Theta(\bar{a}) \in \left(\frac{r-\rho}{2},\, \frac{r+\rho}{2}\right), \qquad \lambda_R^* < \lambda_I^* \text{ for all binding floors.}$$

9 Conclusion

This paper studies a simple and common policy instrument, namely a minimum slaughter age or weight rule that postpones harvest along the maturity margin. We embed the rule in a continuous-time model of cattle as biological capital. The framework delivers closed-form steady states for the unconstrained benchmark and for the binding-floor regime, and it characterizes the transition once the rule is removed. The central message is that timing floors shift mass from flow to stock. They enlarge the standing herd, they lower the marginal value of an additional unit of biomass, and they shape sustainable output in a way that depends on the tightness of the floor.

Two findings matter for policy. First, moderate floors can raise long-run beef supply by leveraging a larger herd, even though animals are slaughtered less often. Tightening the floor further reverses this effect and reduces sustainable throughput despite heavier carcasses at harvest. Second, removing a binding floor produces a sharp, short-run jump in slaughter, driven by the backlog of over-mature animals and a temporary reduction in the chosen slaughter age, followed by a monotone return of the herd and the shadow value to their interior levels.

The analysis is deliberately transparent and rests on two primitives. The first is an Euler equation that pins down the interior stock from biology and discounting. The second is a harvest fraction that declines with slaughter age because within-animal weight growth exhibits diminishing returns. Under these conditions, the steady-state comparisons are robust to alternative preferences, biological growth, age-specific survival, and simple holding costs. The model remains portable to other maturity-based rules while retaining enough structure to map cleanly to the cattle setting.

The framework also yields measurement objects. The wedge between marginal utility and the shadow value summarizes the dynamic efficiency cost of a binding floor and can be calibrated with a growth moment for the herd, a minimal description of within-animal weight gain, and a discount rate. Policy changes that tighten or relax slaughter thresholds generate clear predictions. In particular: (i) tightening the floor raises sustainable throughput if and only if the status-quo harvest fraction exceeds the MSY benchmark $r/2$, and lowers it otherwise (cf. $\partial c_R^*/\partial \bar{a}$ in (21)); and (ii) full repeal raises long-run throughput if and only if the pre-repeal rule was sufficiently tight, $\Theta(\bar{a}) < (r-\rho)/2$, and lowers it otherwise (Proposition 5). These contrasts can be taken to administrative records on slaughter weights and ages or to micro-level panel data on lots moving through finishing.

Two limitations suggest next steps. We abstract from endogenous prices and financing, which would transmit timing rules across markets and reshape the transition. Embedding the sector in general equilibrium is therefore a natural extension. We also assume perfect enforcement and homogeneous producers. Heterogeneity in compliance and technology would sharpen identification and inform incidence by clarifying who bears the wedge and who benefits from larger herds. Exploring these margins, and testing the predictions around actual policy changes, would deepen our understanding of maturity-based regulation in livestock and related settings.

Taken together, the results point to a pragmatic view. Where maturity-based regulation serves objectives outside the planner's problem, such as animal-welfare standards, product quality, or political feasibility, the formulas here offer a tractable way to quantify the dynamic cost. Where those objectives are absent, the efficiency case favors removing binding floors. Doing so raises welfare, eliminates the wedge, and returns the system to the first best. These conclusions rest on measurable primitives and on mechanisms that yield testable predictions.

References

Amaro, Isabel Benito, "Análisis de la Resolución de Peso Mínimo de Faena," *Revista Argentina de Economía Agraria*, 2024, *24* (1), 28–41.

Amer, P., R. Kemp, J. Buchanan-Smith, G. Fox, and C. Smith, "A Bioeconomic Model for Comparing Beef Cattle Genotypes at Their Optimal Economic Slaughter End Point," *Journal of Animal Science*, 1994, *72*, 38–50.

Arnade, Carlos and Keithly Jones, "Modeling the Cattle Replacement Decisions," in "2003 Annual Meeting of the American Agricultural Economics Association" Montreal, Canada 2003. AgEcon Search working paper, paper 21960.

Clark, Colin W., *Mathematical Bioeconomics: The Mathematics of Conservation*, 3 ed., Hoboken, NJ: Wiley-Blackwell, 2010.

Faustmann, Martin, "Berechnung des Werthes, welchen Waldboden, sowie noch nicht haubare Holzbestände für die Waldwirtschaft besitzen," *Allgemeine Forst- und Jagd-Zeitung*, 1849, *15*, 441–455.

Foster, K. A. and O. R. Burt, "A Dynamic Model of Investment in the U.S. Beef-Cattle Industry," *Journal of Business & Economic Statistics*, 1992, *10* (4), 419–426.

Frasier, W. Marshall and George H. Pfeiffer, "Optimal Replacement and Management Policies for Beef Cows," *American Journal of Agricultural Economics*, 1994, *76* (4), 847–858.

Jarvis, Lovell S., "Cattle as Capital Goods and Ranchers as Portfolio Managers: An Application to the Argentine Cattle Sector," *Journal of Political Economy*, 1974, *82* (3), 489–520.

Kamien, Morton I. and Nancy L. Schwartz, *Dynamic Optimization: The Calculus of Variations and Optimal Control in Economics and Management*, 2 ed., Amsterdam: North-Holland, 1991.

Kim, K., J.-S. Lee, Y. Oh, S. Kang, S. C. Lee, W. Park, and Y. Ko, "The Optimal TDN Levels of Concentrates and Slaughter Age in Hanwoo Steers," *Journal of Animal Science and Technology*, 2005, *47* (5), 731–744.

Lee, S. and J. Lee, "Estimates of an Optimal Slaughter Age in Regard to Considerations of Carcass Traits and Production Costs in Hanwoo Steer," *Journal of the Korea Academia-Industrial Cooperation Society*, 2024. Unable to verify volume/issue/pages online; please confirm with your copy.

Lee, S.-C., H.-H. Choi, J.-S. Shin, K. Kim, Y. Oh, and D. Cheon, "Carcass Characteristics and Profitability Analysis Based on Slaughter Age of Hanwoo Steers," *Journal of Animal Science and Technology*, 2013, *55* (4), 315–323.

López-Campos, Óscar, Jennifer L. Aalhus, Erasmus K. Okine, Vern S. Baron, and John A. Basarab, "Effects of Calf- and Yearling-Fed Beef Production Systems and Growth Promotants on Production and Profitability," *Canadian Journal of Animal Science*, 2013, *93* (1), 171–184.

Melton, B. E., "Economics of Beef Cow Culling and Replacement Decisions under Genetic Progress," *Western Journal of Agricultural Economics*, 1980, *5* (1), 137–147.

Meng, Xiang, Niklas L. P. Lundström, Mats Bodin, and Åke Brännström, "Dynamics and Management of Stage-Structured Fish Stocks," *Bulletin of Mathematical Biology*, 2013, *75* (1), 1–23.

Płotkowski, Łukasz, S. Zając, E. Wysocka-Fijorek, A. Gruchała, J. Piekutin, and S. Parzych, "Economic Optimization of the Rotation Age of Stands," *Folia Forestalia Polonica, Series A – Forestry*, 2016, *58* (2), 67–75.

Pordomingo, Aníbal J. and Adriana B. Pordomingo, "Effects Backgrounding-Finishing Programs of Different Age/Weight at Harvest of Feedlot Steers," *Meat Science*, 2021, *177*, 108493.

Rosen, Sherwin, "Dynamic Animal Economics," *American Journal of Agricultural Economics*, 1987, *69* (3), 547–557.

_ , Kevin M. Murphy, and Jose A. Scheinkman, "Cattle Cycles," *Journal of Political Economy*, 1994, *102* (3), 468–492.

Rossini, Gustavo, Rodrigo García Arancibia, and Edith Depetris Guiguet, "Argentine Government Policies: Impacts on the Beef Sector," *Agricultural and Food Economics*, 2017, *5* (1), 1–14.

Rucker, R. R., O. R. Burt, and J. T. LaFrance, "An Econometric Model of Cattle Inventories," *American Journal of Agricultural Economics*, 1984, *66* (2), 131–144.

Schmitz, John D., "Dynamics of Beef Cow Herd Size: An Inventory Approach," *American Journal of Agricultural Economics*, 1997, *79* (2), 532–542.

Schott, Stephan, "The Optimal Selection and Harvest of Multiple Cohorts," *Marine Resource Economics*, 2001, *16* (2), 109–126.

Seierstad, Atle and Knut Sydsæter, *Optimal Control Theory with Economic Applications*, Amsterdam: North-Holland, 1987.

Stewart, H. M., E. B. Burnside, J. W. Wilton, and W. C. Pfeiffer, "A Dynamic Programming Approach to Culling Decisions in Commercial Dairy Herds," *Journal of Dairy Science*, 1977, *60* (4), 602–617.

Stokey, Nancy L., Jr. Lucas Robert E., and Edward C. Prescott, *Recursive Methods in Economic Dynamics*, Cambridge, MA: Harvard University Press, 1989.

Tahvonen, Olli, "Optimal Harvesting of Age-Structured Fish Populations," *Marine Resource Economics*, 2009, *24* (2), 147–169.

Trapp, James N., "Investment and Disinvestment Principles with Nonconstant Prices and Varying Firm Size Applied to Beef-Breeding Herds," *American Journal of Agricultural Economics*, 1986, *68* (3), 691–703.

Tronstad, Russell and Russell Gum, "Cow Culling Decisions Adapted for Management with CART," *American Journal of Agricultural Economics*, 1994, *76* (2), 237–249.

Wan, F. Y. M. and K. Anderson, "Optimal Forest Harvesting with Ordered Site Access," *Studies in Applied Mathematics*, 1983, *68* (3), 189–226.

Williams, C. B. and G. L. Bennett, "Application of a Computer Model to Predict Optimum Slaughter End Points for Different Biological Types of Feeder Cattle," *Journal of Animal Science*, 1995, *73* (4), 1029–1039.

Yager, William A., R. Clyde Greer, and Oscar R. Burt, "Optimal Policies for Marketing Cull Beef Cows," *American Journal of Agricultural Economics*, 1980, *62* (3), 456–467.

A Exact Age-Structured Transitional Dynamics

Let $n(t,u)$ denote the density of heads of age u at time t (heads per unit age). Individuals age at unit speed, face no natural mortality (for clarity), and are harvested deterministically upon reaching a time-varying slaughter age $a(t)$.

Age transport and absorbing boundary. The age density obeys the McKendrick–von Foerster equation

$$\partial_t n(t,u) + \partial_u n(t,u) = 0, \quad 0 < u < a(t), \qquad n(t,0) = b(t), \tag{32}$$

where $b(t) \geq 0$ is the entry (birth) flow. The surface $u = a(t)$ is absorbing: heads are removed upon crossing it.

Biomass stock and boundary flux. Let $w(u)$ be live weight at age u with $w(0) = 0$ and $w'(u) > 0$. Biomass and the *continuous* outflow for t at which $a(\cdot)$ is continuous are

$$x(t) = \int_0^{a(t)} w(u)\, n(t,u)\, du, \qquad c(t) = w\Big(a(t)\Big)\, \Big(1 - \dot{a}(t)\Big)_+\, n\Big(t, a(t)^-\Big), \tag{33}$$

i.e., the biomass-weighted flux through the moving boundary; $(z)_+ = \max\{z, 0\}$.

Mass balance. Using (32) and integration by parts (with a moving upper limit),

$$\dot{x}(t) \;=\; \int_0^{a(t)} w'(u)\, n(t,u)\, du \;+\; w\Big(a(t)\Big)\, n\Big(t, a(t)^-\Big)\, \Big(\dot{a}(t) - 1\Big).$$

Define the net boundary flux $c^{\text{net}}(t) \equiv w(a(t))\Big(1 - \dot{a}(t)\Big)\, n(t, a(t)^-)$. Then

$$\dot{x}(t) \;=\; \int_0^{a(t)} w'(u)\, n(t,u)\, du \;-\; c^{\text{net}}(t).$$

When $1 - \dot{a}(t) \geq 0$ (as in our reform, where the threshold initially moves down and is later held fixed), $c^{\text{net}}(t)$ coincides with the outflow $c(t)$ in (33), so $\dot{x} = \int_0^{a(t)} w' n - c$ holds exactly on our paths.

Backlog at a downward jump in the threshold. If a has a downward jump at $t = t_0$, the instantaneous biomass removed equals

$$\Delta x \;=\; \int_{a(t_0^+)}^{a(t_0^-)} w(u)\, n(t_0^-, u)\, du. \tag{34}$$

Under the pre-repeal steady state with constant $\bar{a}$ and constant entry b^*, $n(t_0^-, u) \equiv b^*$ on $[0, \bar{a}]$, so $\Delta x = b^* \int_{a(t_0^+)}^{\bar{a}} w(u)\, du$, and $x(t_0^+) = x(t_0^-) - \Delta x$.

Stationary benchmark as a special case. If $a(t) \equiv a$ and $b(t) \equiv b$, the stationary solution is $n(u) \equiv b$ on $[0, a]$. Then $x = b \int_0^a w$, $c = b\, w(a)$, and $c/x = w(a)/\int_0^a w = \Theta(a)$ as in the main text.

Wash-in under a fixed policy. If from some date onward $a(t) \equiv a^*$ and $b(t) \to b^*$, then $n(t, \cdot) \to b^*$ on $[0, a^*]$ along characteristics within at most a^* units of time, so $c(t) = x(t)\, \Theta(a^*)$ holds exactly thereafter.

B Monotonicity of the Harvest Fraction for the Canonical Curve

This appendix provides a direct proof for the canonical case and thereby exemplifies Proposition 1.

Proof of Proposition 1. With $w(a) = \frac{\alpha a}{a+k}$ and $D(a) \equiv \int_0^a w(u)\, du = \alpha\Big[a - k \ln(1 + \frac{a}{k})\Big]$, write $\Theta(a) = \frac{w(a)}{D(a)}$. Then

$$\Theta'(a) = \frac{w'(a) D(a) - w(a)^2}{D(a)^2}.$$

A direct calculation gives

$$w'(a) D(a) - w(a)^2 \;=\; \frac{\alpha^2}{(a+k)^2}\Big(- a^2 + k\Big[a - k \ln\Big(1 + \tfrac{a}{k}\Big)\Big]\Big).$$

Let $x \equiv a/k > 0$. Then

$$w'(a) D(a) - w(a)^2 \;=\; -\frac{\alpha^2 k^2}{(a+k)^2} \underbrace{\Big(x^2 - x + \ln(1+x)\Big)}_{\equiv\, g(x)}.$$

It suffices to show $g(x) > 0$ for all $x > 0$. Note $g(0) = 0$, $g'(x) = 2x - 1 + \frac{1}{1+x}$, and $g''(x) = 2 - \frac{1}{(1+x)^2} > 0$ for $x > 0$, so g' is strictly increasing with $g'(0) = 0$, whence $g'(x) > 0$ and $g(x) > 0$ for all $x > 0$. Therefore $w'(a) D(a) - w(a)^2 < 0$ and $\Theta'(a) < 0$ for all $a > 0$. □

Remark 4. This canonical case also follows from the general sufficient condition in Appendix H.5: any increasing, concave w with $w(0) = 0$ implies $\Theta'(a) < 0$.

C Capital Deepening: $x_R^* > x_I^*$ iff $\Theta(\bar{a}) < \frac{r+\rho}{2}$

Lemma 2. Let $x_I^* = \frac{K}{2}(1-\rho/r)$ be the interior stock and $x_R^* = K(1-\Theta(\bar{a})/r)$ the regulated stock. Then

$$x_R^* > x_I^* \quad \Longleftrightarrow \quad \Theta(\bar{a}) < \frac{r+\rho}{2}.$$

Proof. Subtract: $x_R^* - x_I^* = K\Big(1-\Theta(\bar{a})/r\Big) - \frac{K}{2}\Big(1-\rho/r\Big) = \frac{K}{2r}\Big(r+\rho-2\Theta(\bar{a})\Big)$. The RHS is positive iff $\Theta(\bar{a}) < \frac{r+\rho}{2}$. □

Remark 5. Because $\Theta(\cdot)$ is strictly decreasing (Appendix B), $\Theta(\bar{a}) < \Theta(a^*) = \frac{r+\rho}{2}$ holds exactly when the floor binds: $\bar{a} > a^*$.

D Shadow Value: $\lambda_R^* < \lambda_I^*$ When the Floor Binds

Lemma 3. If $\bar{a} > a^*$ (binding floor), then $\lambda_R^* < \lambda_I^*$.

Proof. At the regulated steady state,

$$\lambda_R^* = \frac{\sqrt{\Theta(\bar{a})}}{2\sqrt{x_R^*}\,[\rho + r - \Theta(\bar{a})]} < \frac{1}{2\sqrt{x_R^*\,\Theta(\bar{a})}},$$

because $\rho + r - \Theta(\bar{a}) > \Theta(\bar{a})$ when $\Theta(\bar{a}) < \frac{r+\rho}{2}$ (binding). Since $\Theta(\bar{a}) < \Theta(a^*)$ and $x_R^* > x_I^*$ (Appendix C),

$$\frac{1}{2\sqrt{x_R^*\,\Theta(\bar{a})}} < \frac{1}{2\sqrt{x_R^*\,\Theta(a^*)}} \le \frac{1}{2\sqrt{x_I^*\,\Theta(a^*)}} = \lambda_I^*.$$

□

E Throughput Comparison $c_R^* \gtrless c_I^*$

Proof of Proposition 5. Write $c_R^* = K\Big[\Theta - \Theta^2/r\Big]$ with $\Theta \equiv \Theta(\bar{a})$ and $c_I^* = \frac{K}{4r}(r^2-\rho^2)$. Then

$$c_R^* > c_I^* \iff 4\Theta^2 - 4r\Theta + (r^2-\rho^2) \;<\; 0.$$

The quadratic on the left has roots $\Theta = \frac{r\pm\rho}{2}$; therefore $c_R^* > c_I^*$ iff $\Theta \in \Big(\frac{r-\rho}{2}, \frac{r+\rho}{2}\Big)$, with equality at the endpoints and the reverse inequality outside the interval. □

F Headcount Comparison for the Canonical Curve

Lemma 4. Under $w(u) = \frac{\alpha u}{u+k}$ and a uniform age profile, if $\bar{a} > a^*$ then $N_R^* > N_I^*$.

Proof. Use $\overline{w}(a) = \alpha\Big[1 - \frac{k}{a}\ln(1+\frac{a}{k})\Big]$ and the identity

$$\overline{w}(a) = \frac{\alpha}{(a+k)\,\Theta(a)} \quad \text{(Appendix A)}.$$

Headcount at a steady state with slaughter age a equals $N(a) = x^*(a)/\overline{w}(a)$. Under regulation, $x_R^*(a) = K(1 - \Theta(a)/r)$. Hence

$$N(a) = \frac{K}{\alpha}\Big(1 - \frac{\Theta(a)}{r}\Big)(a+k)\,\Theta(a) \;\equiv\; F(a).$$

Differentiating,

$$F'(a) = \Theta(a)\Big(1 - \frac{\Theta(a)}{r}\Big) + (a+k)\,\Theta'(a)\Big(1 - \frac{2\Theta(a)}{r}\Big).$$

At $a = a^*$, $\Theta(a^*) = \frac{r+\rho}{2}$ implies $1 - \frac{2\Theta(a^*)}{r} = -\rho/r < 0$; with $\Theta'(a^*) < 0$ (Appendix B), we get $F'(a^*) > 0$. Since $\Theta'(a) < 0$ and $1 - \frac{2\Theta(a)}{r}$ changes sign only at $\Theta = \frac{r}{2}$, standard arguments show F increases on (a^*, ∞). Therefore, for any binding floor $\bar{a} > a^*$ we have $N_R^* = F(\bar{a}) > F(a^*) = N_I^*$. □

G Additional Proofs and Stability (for Section 7)

G.1 Proof of Proposition 2 (first–best characterization)

Impose the interior FOC $\lambda = 1/(2\sqrt{c})$ and $c = x\,\Theta(a)$. The costate equation (9) reduces to (10), so a steady state satisfies $\rho = r(1 - 2x/K)$, giving $x_I^* = \frac{K}{2}(1 - \rho/r)$ whenever $r > \rho$. With $\dot{x} = 0$ in (11), $r(1 - x_I^*/K) = \Theta(a^*)$, hence $\Theta(a^*) = (r+\rho)/2$. Then $c_I^* = x_I^*\Theta(a^*) = \frac{K}{4r}(r^2 - \rho^2)$ and $\lambda_I^* = \frac{1}{2\sqrt{c_I^*}}$.

G.2 Proof of Proposition 3 (regulated steady state)

With $a(t) \equiv \bar{a}$, $\dot{x} = rx(1 - x/K) - x\,\Theta(\bar{a})$ is strictly concave in x and crosses zero exactly once on $(0, K)$ when $\Theta(\bar{a}) \in (0, r)$, yielding $x_R^* = K(1 - \Theta(\bar{a})/r)$. Then $c_R^* = x_R^*\Theta(\bar{a})$. Setting $\dot{\lambda} = 0$ in (9) and using $r(1 - 2x_R^*/K) - \Theta(\bar{a}) = -rx_R^*/K$ gives $(\rho + \frac{rx_R^*}{K})\lambda_R^* = \Theta(\bar{a})/(2\sqrt{c_R^*})$, hence (19). Limits as $\Theta(\bar{a}) \downarrow 0$ and $\uparrow r$ are immediate.

G.3 Proofs for transitions (Propositions 8 and 9)

Proof of Proposition 8. The absorbing boundary implies that a downward jump in a at $t = 0$ removes the backlog $\Delta x = b^* \int_{a(0^+)}^{\bar{a}} w(u)\,du$, yielding $x(0^+) = x(0^-) - \Delta x$ (Appendix **??**). For $t \geq 0^+$, the interior FOC $u'(c) = \lambda$ holds; under $u(c) = \sqrt{c}$, $\lambda = 1/(2\sqrt{c})$. In the absence of a discrete jump cost at repeal, the current-value costate is continuous, so $\lambda(0^+) = \lambda_R^*$ and $c(0^+) = 1/(4\lambda_R^{*2})$. Because a binding floor implies $\lambda_R^* < 1/(2\sqrt{c_R^*})$ and $\lambda_R^* < \lambda_I^*$ (Proposition 4), we obtain $c(0^+) > c_R^*$ and $c(0^+) > c_I^*$. Finally, evaluate $\partial H/\partial a = x\,\Theta'(a)\big(\frac{1}{2\sqrt{c}} - \lambda\big)$ at $a = a^*$ with $(x, \lambda) = (x(0^+), \lambda_R^*)$; since $\frac{1}{2\sqrt{c(0^+)}} > \lambda_R^*$ and $\Theta'(a^*) < 0$, we have $\partial H/\partial a|_{a=a^*} < 0$, so $a(0^+) < a^*$.

Stable-arm landing. Under the interior FOC, the costate equation is $\dot{\lambda} = \lambda(\rho - r(1 - 2x/K))$. Linearizing the (x, λ) system around (x_I^*, λ_I^*) (Appendix G.4) yields a saddle with a locally downward-sloping stable arm. Given $\lambda(0^+) = \lambda_R^* < \lambda_I^*$, the unique point on the stable arm with that co-state satisfies $x(0^+) > x_I^*$. The planner chooses $a(0^+)$ (hence Δx) so that $(x(0^+), \lambda(0^+))$ lies on that stable arm, ensuring the present-value transversality condition.

Proof of Proposition 9. Along the interior path, $\dot{\lambda} = \lambda(\rho - r(1 - 2x/K))$. Since $x(0^+) > x_I^*$, we have $\dot{\lambda}(t) > 0$ until λ reaches λ_I^*; by the saddle property, $(x(t), \lambda(t))$ remains on the stable arm and converges monotonically to (x_I^*, λ_I^*). Differentiating $\lambda = 1/(2\sqrt{c})$ gives $\lambda\,\dot{c} = -2c\,\dot{\lambda}$, so

$$\dot{c}(t) = -\,2\,c(t)\Big[\rho - r\Big(1 - \frac{2x(t)}{K}\Big)\Big] < 0 \qquad \text{for all } t \geq 0, \tag{35}$$

with $\dot{c}(t) \to 0$ as $x(t) \to x_I^*$. This proves monotone decline of $c(t)$ to c_I^*.

G.4 Local stability (saddle property) for interior and regulated steady states

Interior. Write the system in (x, λ) under the interior FOC:

$$\dot{x} = rx\Big(1 - \frac{x}{K}\Big) - \frac{1}{4\lambda^2}, \qquad \dot{\lambda} = \lambda\Big(\rho - r + \frac{2r}{K}x\Big).$$

At (x_I^*, λ_I^*), the Jacobian is

$$J_I = \begin{pmatrix} r(1 - 2x_I^*/K) & \frac{1}{2}\lambda_I^{-3} \\ \frac{2r}{K}\lambda_I & \rho - r + 2rx_I^*/K \end{pmatrix} = \begin{pmatrix} \rho & \frac{1}{2}\lambda_I^{-3} \\ \frac{2r}{K}\lambda_I & 0 \end{pmatrix},$$

since $r(1 - 2x_I^*/K) = \rho$. Thus $\det J_I = -\frac{r}{K}\lambda_I^{-2} < 0$ and $\operatorname{tr} J_I = \rho > 0$, implying one positive and one negative eigenvalue (saddle).

Regulated. With $a \equiv \bar{a}$, $\dot{x} = f(x) = rx(1 - x/K) - x\Theta(\bar{a})$ and

$$\dot{\lambda} = \rho\lambda - \frac{\Theta(\bar{a})}{2\sqrt{x\,\Theta(\bar{a})}} - \lambda\Big[r\Big(1 - \frac{2x}{K}\Big) - \Theta(\bar{a})\Big].$$

At (x_R^*, λ_R^*), $f'(x_R^*) = r(1 - 2x_R^*/K) - \Theta(\bar{a}) = -rx_R^*/K < 0$ and

$$\frac{\partial\dot{\lambda}}{\partial\lambda}\Big|_{(x_R^*, \lambda_R^*)} = \rho - \Big[r\Big(1 - \frac{2x_R^*}{K}\Big) - \Theta(\bar{a})\Big] = \rho + \frac{rx_R^*}{K} > 0.$$

Because $\partial\dot{x}/\partial\lambda = 0$ and $\partial\dot{\lambda}/\partial x > 0$, the Jacobian has negative determinant and mixed-sign eigenvalues (saddle).

G.5 Monotonicity of $\lambda_R^*(\Theta)$ (for Section 4.2)

Lemma 5 (Monotonicity of λ_R^* in Θ). Let $r > 0$, $\rho > 0$, $K > 0$, and define

$$\lambda_R^*(\Theta) = \frac{\sqrt{\Theta}}{2\sqrt{K(1 - \Theta/r)}\,(\rho + r - \Theta)} \qquad \text{for } \Theta \in (0, r).$$

Then $\dfrac{d\lambda_R^*}{d\Theta} > 0$ for all $\Theta \in (0, r)$.

Proof. Take logarithms:

$$\ln \lambda_R^*(\Theta) = \tfrac{1}{2}\ln \Theta - \tfrac{1}{2}\ln\Big(K(1-\Theta/r)\Big) - \ln(\rho + r - \Theta) - \ln 2.$$

Differentiate with respect to Θ:

$$\frac{\lambda_R^{*\prime}(\Theta)}{\lambda_R^*(\Theta)} = \frac{1}{2\Theta} + \frac{1}{2r\left(1-\Theta/r\right)} + \frac{1}{\rho + r - \Theta}.$$

Each term on the right is strictly positive for $\Theta \in (0, r)$ (and $\rho > 0$), hence $\lambda_R^{*\prime}(\Theta)/\lambda_R^*(\Theta) > 0$, which implies $\lambda_R^{*\prime}(\Theta) > 0$. □

G.6 Proof of Proposition 6 (welfare ranking)

Reference note. Throughout this subsection we invoke the envelope theorem for optimal control with parameterized inequality constraints. For background, see Seierstad and Sydsæter (1987), Kamien and Schwartz (1991), and Stokey et al. (1989).

Proof of Proposition 6. (i) *Strict welfare loss.* When $\bar{a} > a^*$, the admissible control set under regulation, $\mathcal{A}_{\text{reg}}(\bar{a}) = \{a(\cdot) : a(t) \geq \bar{a}\ \forall t\}$, is a strict subset of the unconstrained set $\mathcal{A}_{\text{int}}$. Hence the regulated optimum is feasible for the interior problem and $V^*(\bar{a}) \leq V_{\text{int}}^*$. To obtain strictness, recall that along any admissible path the current-value stationarity condition on the control is

$$\frac{\partial H}{\partial a}(t) = x(t)\,\Theta'\Big(a(t)\Big)\,\Big(u'(c(t)) - \lambda(t)\Big).$$

When the floor binds we have $a(t) = \bar{a}$ and, by Kuhn–Tucker, $u'(c(t)) > \lambda(t)$ (strict inequality because $\Theta'(\bar{a}) < 0$ and the floor is strictly binding). Therefore $\frac{\partial H}{\partial a}(t) < 0$ at those dates. Under normality and standard regularity for the Maximum Principle, this strict negativity implies that a small downward perturbation in a (infeasible under the floor but feasible in the interior problem) would raise the Hamiltonian and thus strictly raise the objective. Because the binding set has positive measure when $\bar{a} > a^*$, it follows that $V^*(\bar{a}) < V_{\text{int}}^*$.

(ii) *Welfare monotonicity and envelope.* Consider the parameterized inequality $g(a, \bar{a}) \equiv a - \bar{a} \geq 0$. By the envelope theorem referenced above,

$$\frac{dV^*(\bar{a})}{d\bar{a}} \;=\; \int_0^\infty e^{-\rho t}\,\mu^*(t;\bar{a})\,\frac{\partial g}{\partial \bar{a}}\Big(a^*(t),\bar{a}\Big)\,dt \;=\; -\int_0^\infty e^{-\rho t}\,\mu^*(t;\bar{a})\,dt.$$

Because $\mu^*(t;\bar{a}) \geq 0$ for all t and is strictly positive on a set of positive measure when the floor binds, the derivative is strictly negative.

(iii) *Wedge–bite decomposition.* Along the regulated optimum the KKT conditions give $\frac{\partial H}{\partial a}(t) + \mu^*(t;\bar{a}) = 0$ with $\mu^*(t;\bar{a}) \geq 0$ and $\mu^*(t;\bar{a})\Big(a^*(t) - \bar{a}\Big) = 0$. The current-value Hamiltonian is $H(x, a, \lambda) = u(c) + \lambda\Big(g(x) - c\Big)$ with $c = x\,\Theta(a)$; differentiation yields

$$\frac{\partial H}{\partial a}(t) = x(t)\,\Theta'\Big(a(t)\Big)\,\Big(u'(c(t)) - \lambda(t)\Big).$$

Evaluating at $a(t) = \bar{a}$ when the floor binds and multiplying by -1 gives

$$\mu^*(t;\bar{a}) = -\frac{\partial H}{\partial a}(t) = -\,x(t)\,\Theta'(\bar{a})\,\Big(u'(c(t)) - \lambda(t)\Big),$$

which is strictly positive because $\Theta'(\bar{a}) < 0$ and $u'(c(t)) - \lambda(t) > 0$ at binding. This establishes the stated decomposition and sign. □

Proof of Proposition 7. Let $V(x_0;\bar{a})$ be the value function when $a(t) \geq \bar{a}$ for all $t \geq 0$ and the initial condition is x_0. Consider $g(a,\bar{a}) \equiv a - \bar{a} \geq 0$. Under the standing assumptions (feasibility, normality of the Maximum Principle, and concavity), the envelope theorem referenced above yields the one-sided derivative

$$\frac{\partial V(x_0;\bar{a})}{\partial \bar{a}} \;=\; \int_0^\infty e^{-\rho t}\,\mu^*(t;\bar{a},x_0)\,\frac{\partial g}{\partial \bar{a}}\Big(a^*(t;\bar{a},x_0),\bar{a}\Big)\,dt \;=\; -\int_0^\infty e^{-\rho t}\,\mu^*(t;\bar{a},x_0)\,dt,$$

and integrating from a^* to $\bar{a}$ (and flipping the sign) gives

$$V(x_0;a^*) - V(x_0;\bar{a}) \;=\; \int_{a^*}^{\bar{a}} \left[\int_0^\infty e^{-\rho t}\,\mu^*(t;\tilde{a},x_0)\,dt\right] d\tilde{a},$$

which is (25).

For the sign, along the regulated optimum the KKT condition reads $\frac{\partial H}{\partial a}(t)+\mu^*(t;\tilde{a},x_0) = 0$ with $\mu^* \geq 0$ and complementary slackness. With $H(x,a,\lambda) = u(c) + \lambda\,[g(x) - c]$ and $c = x\Theta(a)$, differentiation gives

$$\frac{\partial H}{\partial a}(t) = x(t)\,\Theta'\Big(a(t)\Big)\,\Big(u'(c(t)) - \lambda(t)\Big).$$

Evaluating at $a(t) = \tilde{a}$ on the binding set and multiplying by -1 yields

$$\mu^*(t;\tilde{a},x_0) = -\,x(t)\,\Theta'(\tilde{a})\,\Big(u'(c(t)) - \lambda(t)\Big) > 0,$$

so the inner integral is strictly positive whenever the floor binds at $\tilde{a}$, and the total gain is strictly positive. □

Proof of Corollary 4. By definition of the value function under a given policy parameter,

$$V(x_0;\bar{a}) \;=\; \int_0^\infty e^{-\rho t}\,u\Big(c^{\text{reg}}(t)\Big)\,dt, \qquad V(x_0;a^*) \;=\; \int_0^\infty e^{-\rho t}\,u\Big(c^{\text{free}}(t)\Big)\,dt.$$

Subtracting yields

$$\Delta V(x_0;\bar{a}\to a^*) \;=\; \int_0^\infty e^{-\rho t}\left[u\Big(c^{\text{free}}(t)\Big) - u\Big(c^{\text{reg}}(t)\Big)\right] dt,$$

which is the claim. Equivalence with the multiplier–integral representation in Proposition 7 follows from the same envelope-theorem argument noted at the start of this subsection and the fundamental theorem of calculus applied over $[a^*,\bar{a}]$. □

H Robustness and Generalizations (for Section 8)

H.1 General instantaneous utility (proof of Proposition 10)

With $H(x,a,\lambda) = u(c) + \lambda[g(x) - c]$ and $c = x\,\Theta(a)$, the interior FOC is $u'(c) = \lambda$. Substituting into the costate equation

$$\dot{\lambda} = \rho\lambda - u'(c)\Theta(a) - \lambda\Big[g'(x) - \Theta(a)\Big]$$

eliminates $\Theta(a)$: $\dot{\lambda} = \rho\lambda - \lambda g'(x)$. The interior steady state solves $g'(x_I^*) = \rho$ and $\Theta(a^*) = g(x_I^*)/x_I^*$; $c_I^* = x_I^*\,\Theta(a^*)$ and $\lambda_I^* = u'(c_I^*)$.

H.2 General concave biological growth (proofs of Propositions 11–12)

Let g be $\mathcal{C}^2$, strictly increasing and strictly concave on $[0, K]$, with $g(0) = g(K) = 0$. Define $h(x) \equiv g(x)/x$ on $(0, K]$ and extend continuously at 0^+. Concavity implies h is strictly decreasing.

Interior. Under $u'(c) = \lambda$, the steady state satisfies $g'(x_I^*) = \rho$ (unique solution) and $\Theta(a^*) = h(x_I^*)$.

Regulated. With $a = \bar{a}$, a positive steady state solves $h(x_R^*) = \Theta(\bar{a})$, which exists uniquely when $\Theta(\bar{a}) \in (0, h(0^+))$.

Comparative statics. If the floor binds, then $\Theta(\bar{a}) < h(x_I^*)$ (since $\bar{a} > a^*$), and by monotonicity of h we have $x_R^* > x_I^*$. For throughput, $c^*(x) = x\,h(x)$ is single-peaked with maximum at the golden-rule stock x^{GR} (where $g'(x^{\mathrm{GR}}) = 0$), so $c_R^* > c_I^*$ iff $h(x_R^*) \in (h(x^{\mathrm{GR}}), h(x_I^*))$, i.e. iff $\Theta(\bar{a}) \in (h(x^{\mathrm{GR}}), h(x_I^*))$. The shadow-value conclusions then follow from $u'(c_R^*) > \lambda_R^*$ and $u'(c_I^*) = \lambda_I^*$.

H.3 Age–specific survival (exponential case)

Let survival be $s(u) = e^{-\mu u}$ with $\mu \geq 0$. For slaughter at age a, biomass and outflow are

$$x = b \int_0^a e^{-\mu u} w(u)\, du, \qquad c = b\, e^{-\mu a} w(a),$$

so the effective harvest fraction is

$$\Theta_\mu(a) \;=\; \frac{e^{-\mu a} w(a)}{\displaystyle\int_0^a e^{-\mu u} w(u)\, du}. \tag{36}$$

Assume w is increasing, concave, and $w(0) = 0$. Then $\Theta'_\mu(a) < 0$ for all $a > 0$.

Proof. Let $D(a) \equiv \int_0^a e^{-\mu u} w(u)\, du$; $D'(a) = e^{-\mu a} w(a)$. Differentiating (36) yields

$$\Theta'_\mu(a) \;=\; \frac{e^{-\mu a}}{D(a)}\Big[w'(a) - \mu w(a)\Big] \;-\; \frac{e^{-2\mu a} w(a)^2}{D(a)^2}.$$

Using $D(a) \geq e^{-\mu a} \int_0^a w(u)\, du = e^{-\mu a} a\, \overline{w}(a)$ and the concavity facts $\overline{w}(a) \geq \frac{1}{2} w(a)$ and $w'(a) \leq \overline{w}(a)/a \leq w(a)/a$, we get

$$\Theta'_\mu(a) \;\leq\; \frac{1}{a\,\overline{w}(a)}\Big[w'(a) - \mu w(a)\Big] - \frac{w(a)}{a\,\overline{w}(a)} \cdot \frac{w(a)}{2\,\overline{w}(a)} \;\leq\; \frac{1}{a\,\overline{w}(a)}\left[\frac{\overline{w}(a)}{a} - \mu w(a) - \frac{w(a)}{2}\right] \;<\; 0,$$

since $\overline{w}(a) \leq w(a)$ and $\mu \geq 0$.

H.4 Holding/feeding costs

With per–period cost $\phi(x)$, the current-value Hamiltonian is $u(c) - \phi(x) + \lambda[g(x) - c]$. The interior FOC remains $u'(c) = \lambda$ and the costate becomes

$$\dot{\lambda} = \rho\lambda - \lambda g'(x) + \phi'(x).$$

At an interior steady state, $g'(x_I^*) = \rho + \phi'(x_I^*)/\lambda_I^*$ with $\lambda_I^* = u'(c_I^*)$. Since $\phi' \geq 0$, x_I^* falls, $\Theta(a^*) = g(x_I^*)/x_I^*$ rises, and optimal slaughter ages fall. The regulated steady-state *levels* (x_R^*, c_R^*) remain determined by g and $\Theta(\bar{a})$, while

$$(\rho - g'(x_R^*) + \Theta(\bar{a}))\,\lambda_R^* \;=\; u'(c_R^*)\,\Theta(\bar{a}) \;-\; \phi'(x_R^*)$$

implies that λ_R^* *decreases* with $\phi'(x_R^*)$.

H.5 Sufficient conditions for $\Theta'(a) < 0$ with general w

Let $w : [0, \infty) \to \mathbb{R}_+$ be $\mathcal{C}^2$, increasing, concave, and $w(0) = 0$. Define

$$\Theta(a) \;\equiv\; \frac{w(a)}{\displaystyle\int_0^a w(u)\,du}\,.$$

Then $\Theta'(a) < 0$ for all $a > 0$.

Proof. Write $D(a) = \int_0^a w(u)\,du$ and $N(a) = w(a)$, so $\Theta = N/D$. Then

$$\Theta'(a) \;=\; \frac{N'(a)D(a) - N(a)^2}{D(a)^2} \;=\; \frac{D(a)\,w'(a) - w(a)^2}{D(a)^2}.$$

Concavity with $w(0) = 0$ implies $w'(a) \leq w(a)/a$ and $D(a) \geq \frac{1}{2}a\,w(a)$, hence

$$D(a)\,w'(a) - w(a)^2 \;\leq\; \Big(\tfrac{1}{2}a\,w(a)\Big)\frac{w(a)}{a} - w(a)^2 \;=\; -\frac{1}{2}w(a)^2 \;<\; 0.$$

Thus $\Theta'(a) < 0$.